CHAPTER – 3

RESULTS & DISCUSSION

PART – I (OXIDATION)

In this chapter, the results of characterization and catalytic activity of metal complexes supported on poly(styrene-divinylbenzene) is described. These polymer supported metal complexes have been examined as catalysts in the epoxidation/oxidation of alkenes, alkanes & alcohols. The chapter includes the results and discussion of :

3.1 Polymer supported Mn(II) amino acid complexes

3.2 Polymer supported Ru(III) amino acid complexes

3.3 Polymer supported Cu(II) amino acid complexes

3.4 Mechanism of oxidation/epoxidation

3.5 Asymmetric epoxidation

3.6 References

3.1. Poly(styrene-divinylbenzene) supported Mn(II) amino acid complexes

The anchoring of an amino acid on to cross-linked chloromethylated poly(styrene-divinylbenzene) and the loading of manganese on to this liganded polymer was carried out as per the sequences shown in **Scheme 3.1.1.** The three catalysts studied are designated as under:

Mn A = 8% Poly(S-DVB)L-val Mn(II) complex

Mn B = 6% Poly(S-DVB)L-val Mn(II) complex

Mn C = 8% Poly(S-DVB)L-ph ala Mn(II) complex

Anchoring of α-Amino acid

The direct attachment of an amino acid residue to chloromethylated poly(styrene-divinylbenzene) resin has previously been accomplished by employing one of the following routes.

(i) Substitution of chlorine by iodine on the chloromethylated polymer followed by reaction with an α-amino acid [1].

(ii) Reaction of amino acid with cross-linked chloromethylated styrene-divinyl benzene co-polymer in presence of sodium iodide and a base such as tertiary amine [2].

(iii) Reaction of chlorosulfonated polystyrene with sodium salt of amino acid [3,4].

Moderate yields were claimed in case of reaction with chlorosulfonated polystyrene [method (iii)] and low yields were noted with .nethods (i) & (ii).

In the present work initial attempts to react the amino acid with chloromethylated poly (S-DVB) in aqueous as well as in methanolic solution including reflux conditions proved unsuccessful. After several screening experiments, the reaction of amino acid and

the resin in presence of pyridine as a base showed encouraging result as it is known to work well in both aqueous as well as in organic solvents [5]. Using slightly more than molar excess of amino acid and pyridine reproducible grafting on the resin could be achieved (**Table 3.1.1.**). Analysis for nitrogen after ligand attachment gave values of 2.56%, 2.46% and 2.34% respectively for **Mn A, Mn B & Mn C**. These correspond to 1.83 mmol and 1.76 mmol of L-valine anchored per gram of **Mn A & Mn B** and 1.67 mmol of L-phenyl alanine anchored per gram of **Mn C**. It is well known that in *non-aqueous* solvents and with *excess* pyridine quaternization of pendant benzylic rests in chloromethylated styrene-divinyl benzene readily occurs [6,7] which was confirmed by a dummy experiment in our case too. However, the reaction of amino acid and a *stoichiometric* amount of pyridine is feasible only in aqueous medium leading to the desired mode of grafting. Quaternization does not take place under these conditions. In these latter conditions pyridine facilitates the attachment through the amine end by *eliminating* HCl as pyridine-hydrochloride salt. Use of pyridine as a base for such displacement reactions is well documented [5]. In another control experiment pyridine was allowed to react with the polymeric support in the absence of amino acid under identical conditions. After the usual work up analysis of the resin treated with pyridine did not show any nitrogen. This indicates that there is no side reaction taking place in presence of pyridine and the observed nitrogen percent in the amino acid grafted resin entirely comes from the anchored amino acid fragment. This was further confirmed by estimation of the free carboxylic groups on the resin which was found to be equivalent to the amino acid loaded. These details are given in the experimental section.

In yet another related experiment efforts for N-functionalization of amino acid using K_2CO_3 in aqueous methanolic solution as described in a previous report was not effective in our case [8]. Further, indirect verification of mode of linkage was arrived at by reacting benzyl chloride with valine giving N-benzyl valine (mp. 255°C) [8,9] which supports that ligand attachment on polymer occurs from the amine end. The probability of C-alkylation [10] of amino acid under these conditions is thus overruled. The overall synthetic protocol is depicted in **Scheme 3.1.1**.

Complex formation

The reaction of Mn(II) acetate with polymer anchored amino acid was conducted in the pH range of 4.3 – 4.5. A maximum Mn loading of up to 1.7 % was obtained (**Table 3.1.1.**). It is known that all amino acids undergo two reversible proton ionization steps, *viz.*

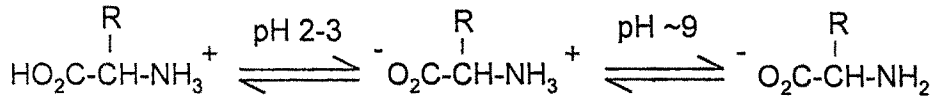

Consequently depending on the solution pH, amino acid can coordinate to metal ion through either or both of amino (NH_2) or carboxyl (CO_2^-) groups. Moreover, the order of stability constants for transition metal ions follows the Irving-Williams series [11]. Thus, for the divalent Mn^{2+} ion with excess amino acid present as employed in our case, it is expected that the formation of a chelate such as Mn(amino acid)$_2$ may be favoured [12]. Based on *p*ka values Gillard *et.al* reported similar (N,O) chelation for different amino acid complexes at lower pH range [13].

Catalyst characterization

Some of the important physical properties of these catalysts have been measured and the data compiled in **Table 3.1.2.** **Mn B** has a slightly higher surface area and larger pore volume than **Mn A** & **Mn C**. Metal loading on **Mn B** with 6% cross-link (Mn 1.7% /gm resin) was slightly higher than in **Mn A** & **Mn C** with 8% cross-link (Mn 1.0% & 0.96% / gm resin respectively) (**Table 3.1.1.**). This result can partly be explained taking into account the fact that with a higher degree of cross-linking (as in **Mn A** & **Mn C**) the polymer network consists of dense and relatively larger number of inaccessible domains leading to lower capacity for metal uptake. The results of swelling behavior (**Table 3.1.3.**) indicate that swellability was higher in polar solvents than in non-polar aliphatic and aromatic hydrocarbon solvents.

In order to ascertain the attachment of amino acid and the metal on the polymer support IR spectra were recorded separately in mid (4000-400cm^{-1}) and far IR (600-30cm^{-1}) regions at different stages of synthesis. The sharp C-Cl peak (due to $-CH_2Cl$ group) at 1261 cm^{-1} in the starting polymer was practically absent or seen as a weak band after introduction of valine on the support. A strong band at 3423 cm^{-1} in poly (S–DVB)-L-valine is assigned to –NH (*sec.* amine) vibration. Medium intensity band due to C-N stretching appears at 1090 cm^{-1} both in the supported ligand and the catalysts. A slight shift in the –NH str. band (~12 cm^{-1}) in supported Mn complex indicates the coordination of 'N' of amino acid to the metal [14]. Representative IR spectra of polymer support and catalyst are shown in **Fig. 3.1.1.** The characteristic absorptions due to ν_{asym} COO^- str. and ν_{sym} COO^- str. of carboxylic group are seen at 1639 cm^{-1} and 1487 cm^{-1} respectively in the ligand as well as in supported Mn catalysts. As the bands due to acetate ion (OAc)

also appear in the same region (1600 – 1450 cm^{-1}) there is a possibility of some overlap of these bands. Very weak bands in the far IR region (350 – 325 cm^{-1}) may be due to ν Mn-N and ν Mn-O vibrations.

Representative diffuse reflectance spectra (650 – 300 nm) of **Mn A** and **Mn B** showed a broad band around 380 nm on a rising tail. No other d-d transitions were observed in the visible region (**Fig. 3.1.2**). Mononuclear Mn(II) complexes (d^5 ion) usually show little or no absorption in the visible region [15,16]. As shown in **Scheme 3.1.1** (structures I & II) the predominant species on the rigid polymer matrix will have bidentate amino acid coordinated to Mn(II) to form a stable poly-Mn(amino acid)$_2$ complex. The other possibility of octahedral configuration though remote, can be visualized by assuming coordination through the two acetate ions.

Scanning electron micrographs (SEM) at various stages of preparation of the polymer supported L-valine and the manganese complexes were recorded to understand morphological changes occurring on the surface of the polymer. Scanning was done at 50-100 μ range across the length of the polymer beads. Comparison of images taken at a magnification of ~$3x10^3$ showed that the smooth spherical surface of the starting poly (S-DVB) (**Fig. 3.1.3a**) is distinctly altered, exhibiting uneven contours on the top layer upon anchoring of the amino acid (**Fig. 3.1.3b**). After metal incorporation, randomly oriented dark depositions on the outer surface of the resin were seen (**Fig. 3.1.3c**). A rough estimate showed that the width of deposit varies from 1.0– 7.5μ.

A single step degradation peak in the TG was observed for the virgin polymer in the 410-440°C temperature range. On the other hand all the three Mn - supported

catalysts degrade at considerably lower temperatures (**Table 3.1.4.**). The variation in cross-linking in **Mn A, Mn C** and **Mn B** however, does not show much deviation in their thermal stabilities as seen from the wt.loss which was around 22-23% at 360-365°C. Some weight loss was also observed at ~100°C due to loosely bound surface moisture or volatiles on the surface of catalysts. These features are depicted in **Fig. 3.1.4**. The early decomposition profile implies either dissociation of covalently bound amino acid ligand moieties or a partial scission of polymeric chain. However, due to hazards associated with hydroperoxides in oxidation reactions, the working temperatures were deliberately kept below 70°C.

The X-band EPR spectrum of **Mn A** recorded in the solid state at room temperature show broad signals and the experimentally calculated 'g' value of 2.0278 is indicative of the presence of mononuclear Mn(II) complex [17]. The unsymmetrical six line hyperfine signals centered at g = 2 is associated with the I = 5/2 nuclear spin of ^{55}Mn. Due to the irregular feature of resonance signals (**Fig. 3.1.5**) the hyperfine coupling constant ^{a}Mn was computed by averaging over all 6 lines and is equal to ~110 G. These are of the same order as found for other mononuclear high spin Mn^{2+} complexes [18,19].

Catalytic evaluation

The ability of the polymer bound Mn(II)-L-valine complexes to catalyze organic reactions was explored by conducting a systematic study on epoxidation of olefins. Substrates such as styrene, norbornylene, *cis*-cyclooctene and cyclohexene were subjected to catalytic epoxidation using **Mn A** and **Mn B** in presence of TBHP as the

terminal oxidant. The catalytic evaluation of **Mn C** for asymmetric epoxidation is discussed in **section 3.5.** Blank experiments revealed that no reaction occurred in the absence of either the catalyst or the oxidant. The results of oxidation carried out at two different temperatures are compiled in **Table 3.1.5.** All compounds undergo epoxidation in presence of the two Mn supported catalysts and in some cases very high selectivities were obtained. In order to verify whether the catalysts operate in a truly heterogeneous manner a simple experiment was performed by keeping the catalyst in contact with the solvent and stirred for 24 h reaction period; the catalyst filtered off and the filtrate examined for any residual catalytic activity. Only trace amount of oxidation product (yield: 0.1% -0.3%) was detected indicating clearly that the observed reactivity was due to the metal complex bound to the polymer support. A second and a more conclusive evidence for heterogeneity was arrived at by following a recent probe suggested by Sheldon [20]. The reaction of styrene with one of the catalyst (**Mn A**) was carried out at 45°C as described in the experimental part. After 3 h the reaction was deliberately intercepted and the catalyst quickly separated by filtering at the same temperature. Analysis of the reaction mixture *at this point* showed a conversion of 9.2%. Stirring was continued for a total of 24h and analysis at the end of this period (*without the catalyst*) showed only a marginal increase in conversion (11.7 %). In contrast, the result of reaction performed for 24h in *presence* of the catalyst indicated around 38% overall conversion (**Table 3.1.5.**).

As a further extension of this probe another set of reaction was performed for 3h *without* the substrate at 45°C, the catalyst quickly filtered off and *then* the substrate added to the filtrate. Stirring was continued for 24h and analysis of reaction mixture showed

only ~2.2% conversion. All the above diagnostic tests unambiguously point to the fact that the catalyst behave in a truly *heterogeneous* manner. Though our results show minor leaching, more importantly, the metal species leached into the filtrate *is not responsible* for the observed catalytic activity.

Epoxidation of styrene results in multiple product formation namely epoxide, benzaldehyde and acetophenone. In this reaction, interestingly aldehyde is the major product rather than the epoxide regardless of the variation in reaction conditions. Expectedly overall yields were higher at 45°C than at 28°C. Formation of benzaldehyde (sel. 86%) as the major product suggests that the reaction with hydroperoxide proceeds beyond the epoxide stage resulting in the oxidative cleavage of styrene [21]. In order to eliminate the possibility whether Mn(II) itself takes part in the rearrangement of intermediate epoxide to PhCHO, a blank experiment was conducted using styrene oxide as the substrate. No PhCHO was found thus corroborating our conclusion that the primary product of styrene oxidation is benzaldehyde. Both norbornylene and *cis*-cyclooctene selectively gave corresponding epoxides, the reaction being more facile with the bicyclic olefin (yield = 30%) than the monocyclic olefin (yield = 9%). Contrary to this, in case of cyclohexene only traces of epoxide was formed though the yields are higher (yield = 45%). However, the reaction in this case is nonselective leading to the formation of products of allylic oxidation. In the examples discussed above **Mn A** showed higher activity compared to **Mn B**. A detailed study was thus undertaken with this catalyst to understand the effect of operating conditions on the epoxidation of styrene and norbornylene as model substrates. The extent of epoxidation observed at different temperatures and catalyst concentrations are presented in **Table 3.1.6.** As can be inferred

from the Table reaction at 45°C are much more rapid than at 28°C at similar levels of catalyst concentrations. Amongst the different solvents studied comparable activity is observed for acetonitrile and methylene chloride. The reason for poor reactivity in methanol is not clear. With regard to the effect of nature of oxidant on epoxidation it was found that TBHP and CHP (Cumene hydro peroxide) were most effective. Practically no oxidation takes place with either molecular oxygen or hydrogen peroxide.

That the activity of the supported catalysts is limited only to the surface bound complex was confirmed by carrying out a dummy experiment at room temperature (28°C) with very *finely powdered* sample of **Mn A** and norbornylene as substrate. The TON was 20. This matches with the TON of 22 obtained while using the non-powdered beads at the same temperature (Ref. **Table 3.1.5.**).

For a proper understanding of the efficacy of the present polymer supported Mn catalysts vis-à-vis its homogeneous counterpart namely Mn(L-valine)$_2$ complex, direct comparison of catalytic activities under optimized reaction conditions is desirable. In the absence of relevant data on oxidations of olefin using homogeneous amino acid-metal catalysts, an attempt was made to generate *in situ* (without isolation) a simple L-valine complex of Mn(II) by mixing the ligand and the metal acetate in 1:2 molar ratio in an aqueous solution at a pH of ~4.1. After a reaction period of 24 h an aliquot of the solution corresponding to a Mn concentration *equal* to that employed in the supported catalyst was taken up for subsequent epoxidation of styrene and norbornylene in presence of TBHP under identical conditions (45°C). The yields were slightly higher than for the supported catalysts (**Table 3.1.5.**) and were found to be 63.0% and 43.6% respectively. A plausible reason for slower rate of reaction exhibited by both the polymer bound

catalysts **Mn A** and **Mn B** may be due to the slower rate of diffusion of olefins into the polymer matrix at the sites where active catalytic species are located [22].

A preliminary kinetic study on the epoxidation of styrene and norbornylene in presence of TBHP at 28°C was investigated up to about 30 h by analyzing aliquots of reaction mixture at regular intervals of time. In **Fig. 3.1.6** is shown a plot of olefin conversions *vs.* reaction time under a fixed oxidant concentration. With both substrates, the conversions increase almost linearly up to about 15 h. The reaction becomes sluggish thereafter but continues even after 24 h.

Catalyst recycling

One of the main objectives of supporting a homogeneous metal complex on to a polymer support is to enhance the life of the resulting catalyst. We have made a preliminary study of the recycling efficiency of **Mn A** using styrene and norbornylene as model substrates. The catalyst was separated from the reaction mixture after each experiment by filtration, washed with solvent and dried carefully before using it in the subsequent run. These results are shown in **Table 3.1.7**. It can be inferred that the catalyst can be recycled at least about four times. However, there is a progressive loss of activity accompanied by diminished yields. Estimation of Mn present in the recycled catalyst after four cycles revealed a lowering in Mn content by about 30-35% than that present at the start of the first cycle. Partial lowering of % Mn can be due to minor loss of catalyst during recovery after every run. As already described the "hot filtration" test (p. 51) showed that the leached Mn species is *inactive* for epoxidation. The activity profile for four successive cycles is depicted in **Fig. 3.1.7**.

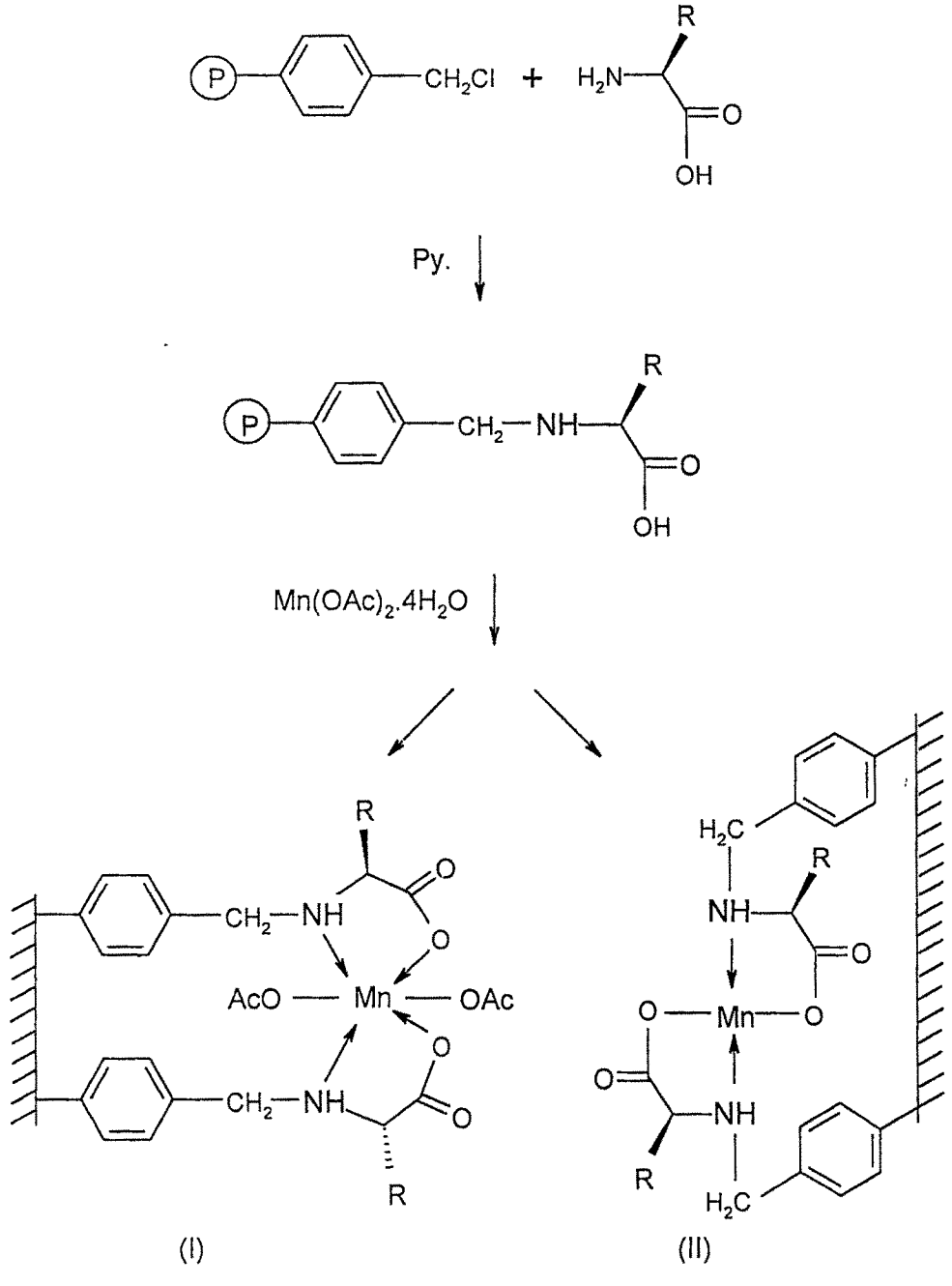

(I) (II)

R = -$CH(CH_3)_2$ for L-val ; R = -CH_2Ph for L-Ph ala

Scheme 3.1.1. Synthesis of poly(S-DVB) supported amino acid Mn(II) complex.

Table 3.1.1. Analytical data of Polymer Support, Ligand and Mn-anchored catalysts

Compound	C%	H%	Cl%	N%	Mn%
8%Poly(S-DVB)CH_2Cl	70.38	5.77	17.56	--	--
6%Poly(S-DVB)CH_2Cl	76.26	6.36	16.14	--	--
8%Poly(S-DVB)-L-val	60.15	5.00	9.47	2.56	--
6%Poly(S-DVB)-L-val	63.28	5.44	9.48	2.47	--
8%Poly(S-DVB)-L-ph ala	62.19	5.59	9.82	2.34	--
Mn A	59.87	5.15	n.d.	2.60	1.00
Mn B	61.54	5.41	n.d.	2.71	1.74
Mn C	61.86	5.93	n.d.	2.37	0.96

n.d. = not determined.

Table 3.1.2. Physical properties of Mn-supported Poly(S-DVB) catalysts

Sample	Surface Area ($m^2 g^{-1}$)	Bulk Density ($g\ cm^{-3}$)	Pore volume ($cm^3 g^{-1}$)
8%Poly(S-DVB)CH_2Cl	32.7	0.44	0.20
6%Poly(S-DVB)CH_2Cl	38.3	0.38	0.29
Mn A	21.9	0.51	0.10
Mn B	33.7	0.45	0.19
Mn C	23.7	0.51	0.12

Table 3.1.3. Swelling data in different solvents (mol %)

Solvent	8% Poly (S-DVB)CH_2Cl	6% Poly (S-DVB)CH_2Cl	**Mn A**	**Mn B**	**Mn C**
Acetonitrile	1.9	2.0	1.4	1.8	1.5
Benzene	1.1	1.1	0.8	0.9	0.8
Dichloromethane	1.5	1.8	1.0	1.4	1.1
Ethanol	1.7	1.9	1.4	1.6	1.4
n-Heptane	0.6	0.6	0.4	0.5	0.4
Methanol	2.7	2.8	2.4	2.4	2.3
Tetrahydrofuran	1.4	1.5	1.0	1.2	0.9
Toluene	1.1	1.1	0.7	0.8	0.7

Table 3.1.4. TG data of polymeric supports and anchored Mn(II) catalysts

Compound	Degr. Temp.(°C)	Wt. loss (%)
8%Poly(S-DVB)CH_2Cl	440	21.0
6%Poly(S-DVB)CH_2Cl	410	21.0
Mn A	119	2.0
	360	22.0
Mn B	102	1.4
	365	23.0
Mn C	110	1.8
	362	22.8

Table 3.1.5. Catalytic oxidation with Mn A and Mn B

Catalyst[a]	Substrate[b]	Temp. (°C)	Yield (%)[c]	Products/ Selectivity (wt. %)				TON[d]
				Epoxide	PhCHO	PhCOMe		
Mn A		28	20.4	7.0	86.4	6.6		38
Mn A	Styrene	45	38.2	19.9	76.5	3.5		71
Mn B		28	34.2	9.2	82.1	8.7		34
Mn B		45	53.0	12.7	87.3	trace		54
Mn A		28	11.1	100.0				22
Mn A	Norbornylene	45	30.6	100.0				60
Mn B		28	10.6	100.0				11
Mn B		45	20.2	100.0				23
Mn A		28	7.3	100.0				15
Mn A	*cis*-cyclooctene	45	9.1	100.0				19
Mn B		45	14.0	100.0				15
				Epoxide	1-one	1-ol	Cy-one	
Mn A		28	43.6	Trace	31.5	48.3	20.0	88
Mn A	Cyclohexene	45	45.4	Trace	28.1	45.5	26.3	93
Mn B		45	39.6	0.4	29.3	39.0	30.2	44

[a] = 0.15 g ; [b] = 5.0 mmol ; [c] = yield based on starting material ; [d] =Turnover number = mmol products/mmol Mn ; 1-one = cyclohexene-1-one ; 1-ol = cyclohexene-1-ol ; Cy-one = cyclohexanone; solvent = acetonitrile.

Table 3.1.6. Epoxidation of styrene & norbornylene by Mn A under different reaction conditions

Parameters	Catalyst wt. (g)	Temp. (°C)	Solvent[c] (20 ml)	Oxidant	TON[d]
	0.15	45	CH_3CN	TBHP	41 (19)
Temp.[a]	0.15	28	CH_3CN	TBHP	24 (6)
	0.15	8-10	CH_3CN	TBHP	Trace (1)
	0.10	45	CH_3CN	TBHP	70 (60)
Catalyst conc.[b]	0.15	45	CH_3CN	TBHP	71 (59)
	0.20	45	CH_3CN	TBHP	69 (54)
	0.15	28	CH_3CN	TBHP	38 (23)
Solvent [b]	0.15	28	CH_2Cl_2	TBHP	36 (26)
	0.15	28	CH_3OH	TBHP	06 (1)
	0.15	28	CH_3CN	H_2O_2	01 (0)
Oxidant [b]	0.15	28	CH_3CN	O_2	0.5 (0)
	0.15	28	CH_3CN	CHP	14 (204)

[a] = reaction time = 8 h; [b] = reaction time = 24 h; [c] = 20 ml; [d] = values in parentheses are for norbornylene; substrate conc. = 5.0 mmol.

Table 3.1.7. Recycling study of Mn A[a]

Cycle no.	Yield (%)[b]	
	styrene	norbornylene
1	37.4	30.1
2	34.0	24.2
3	22.0	18.8
4	17.6	15.0

[a] Conditions: 150 mg catalyst; 10.0 mmol TBHP; 20 ml acetonitrile ; 45°C; 24 h.
[b] Yield based on starting material; 5.0 mmol olefins.

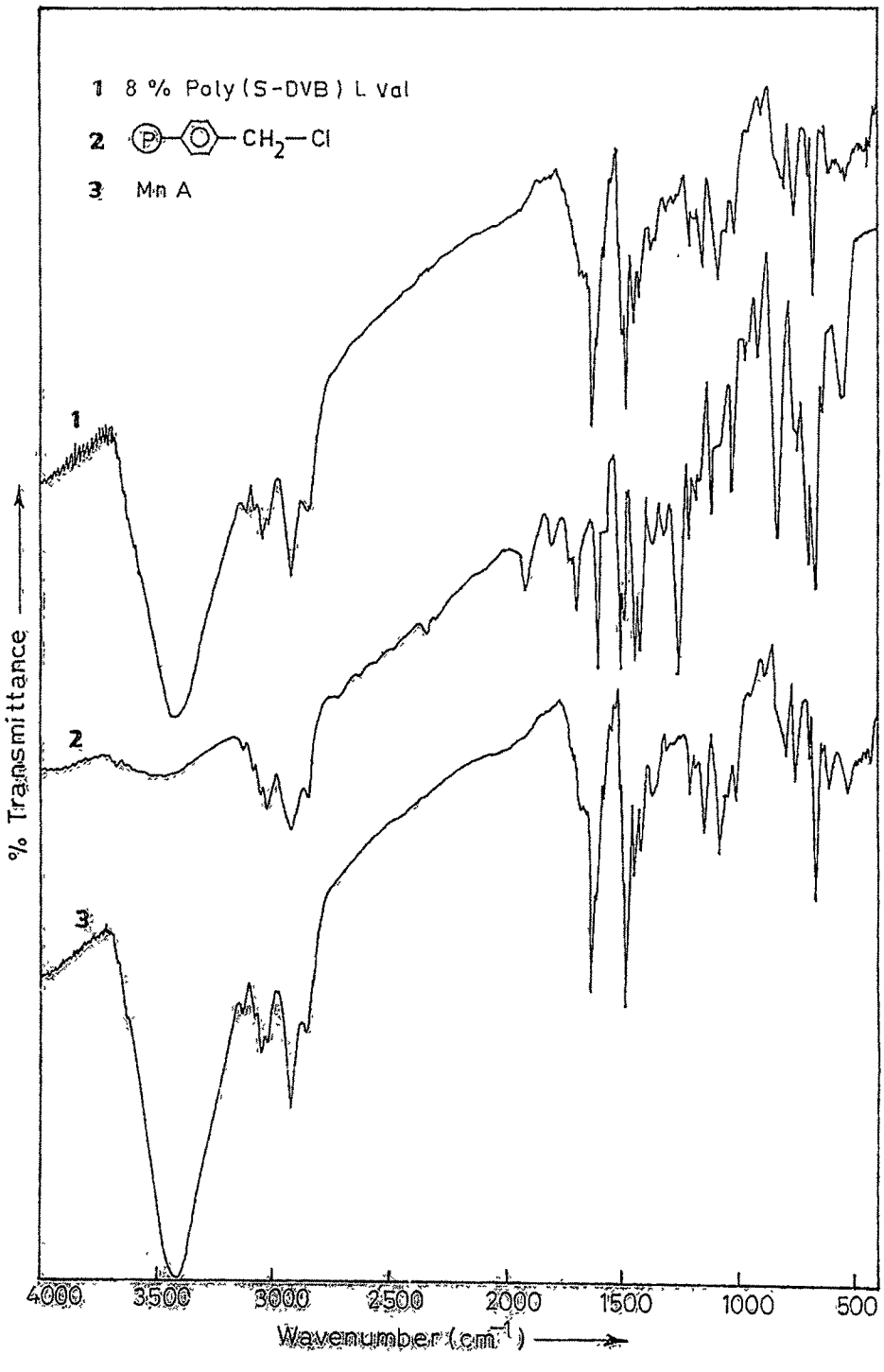

Fig. 3.1.1 FT-IR spectra of support, liganded polymer and catalyst.

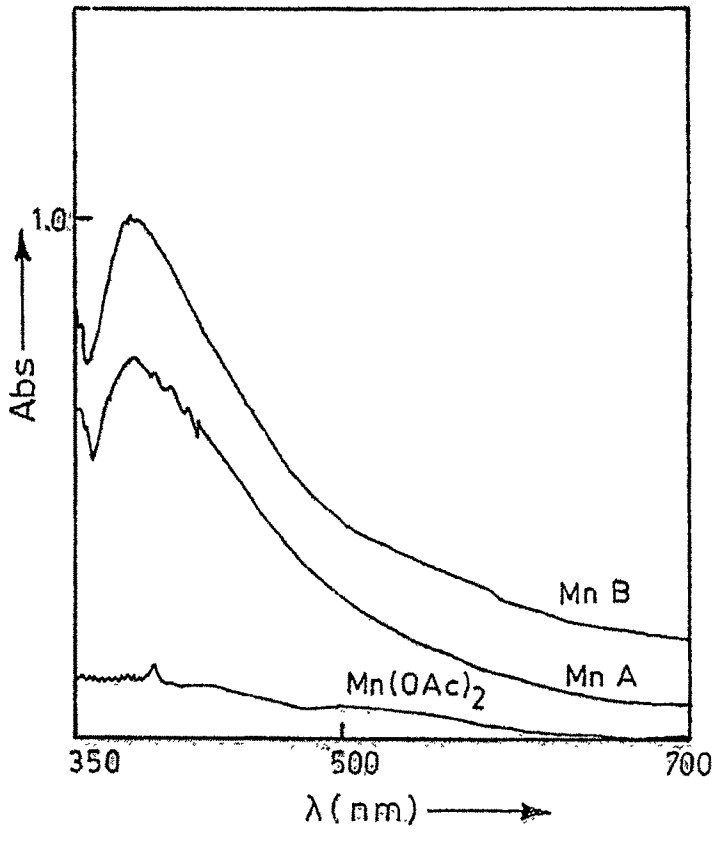

Fig. 3.1.2 Diffuse reflectance spectra of catalysts

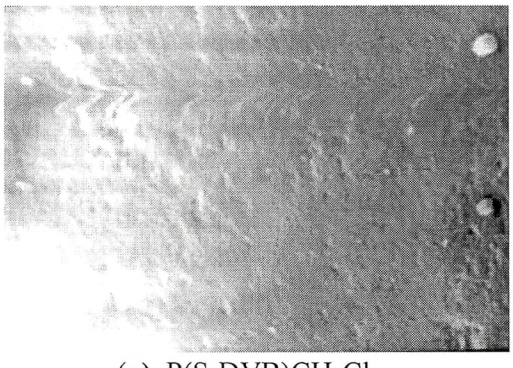

(**a**) P(S-DVB)CH_2Cl

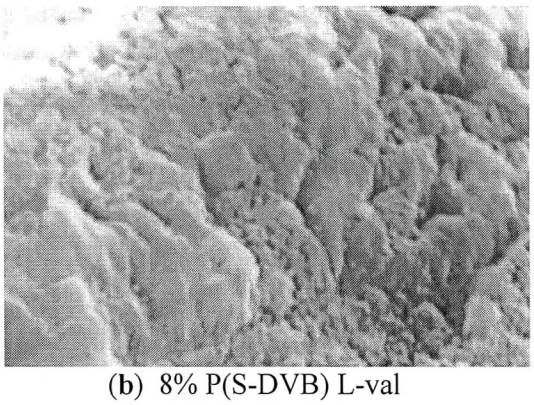

(**b**) 8% P(S-DVB) L-val

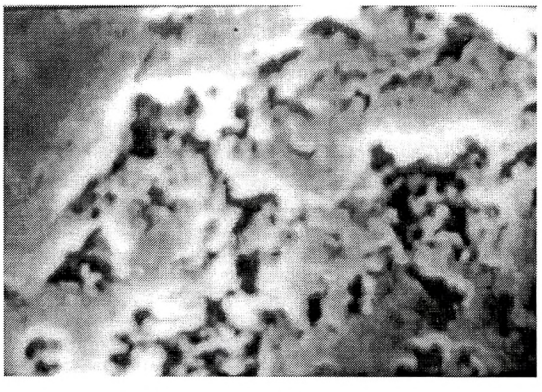

(**c**) **Mn A**

Fig. 3.1.3 Scanning electron micrographs

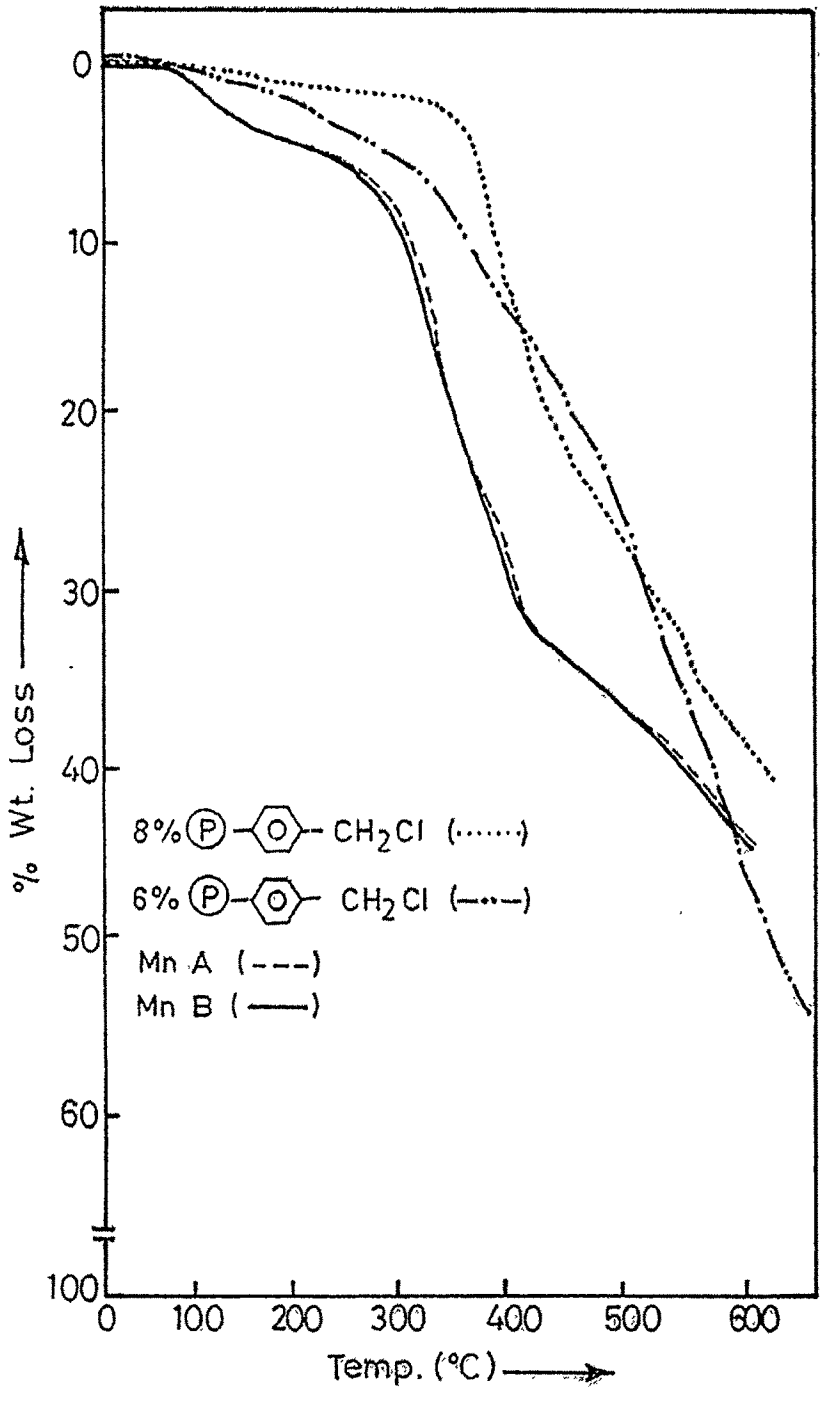

Fig. 3.1.4 TG of support and Mn catalysts..

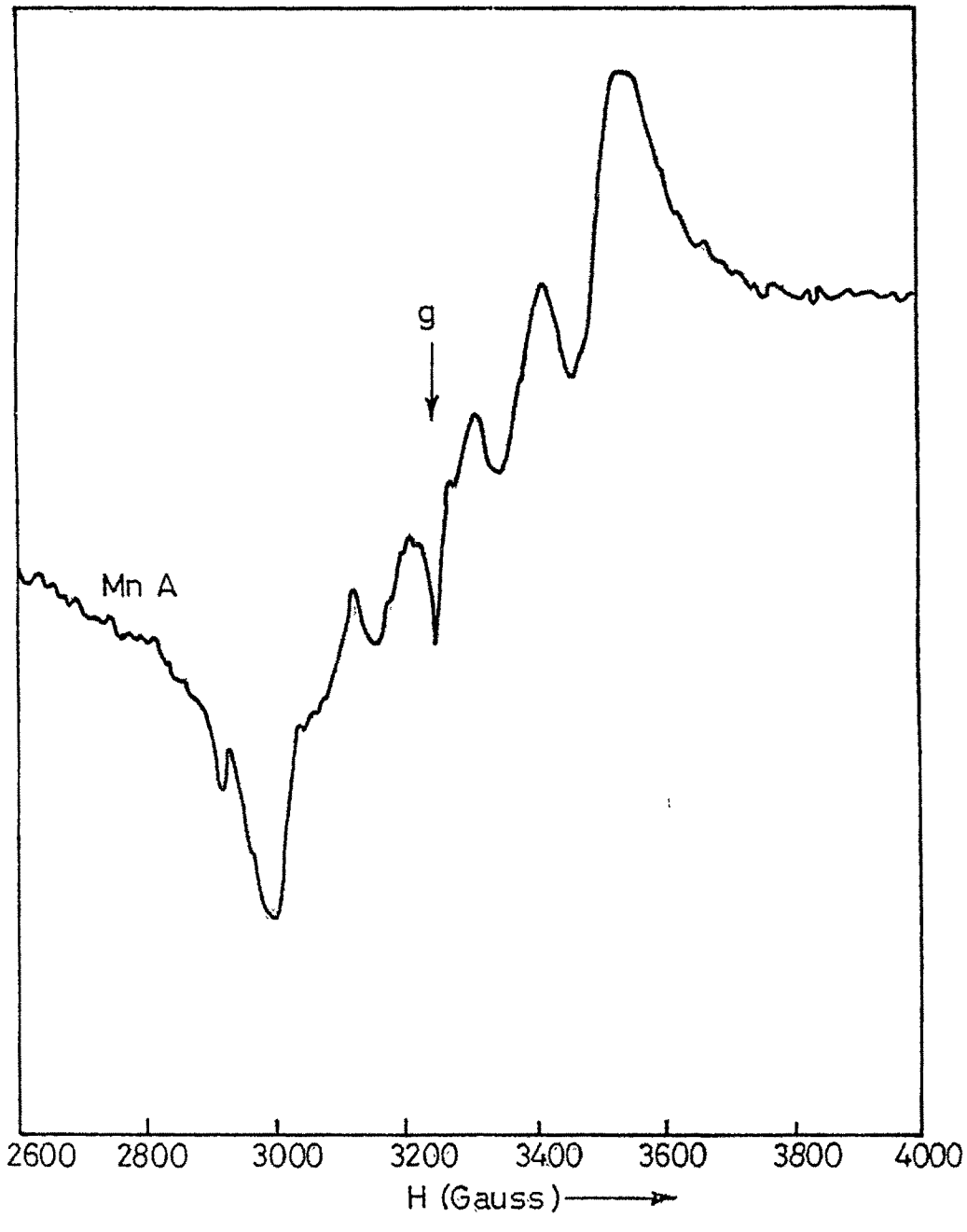

Fig. 3.1.5 ESR spectra of Mn A.

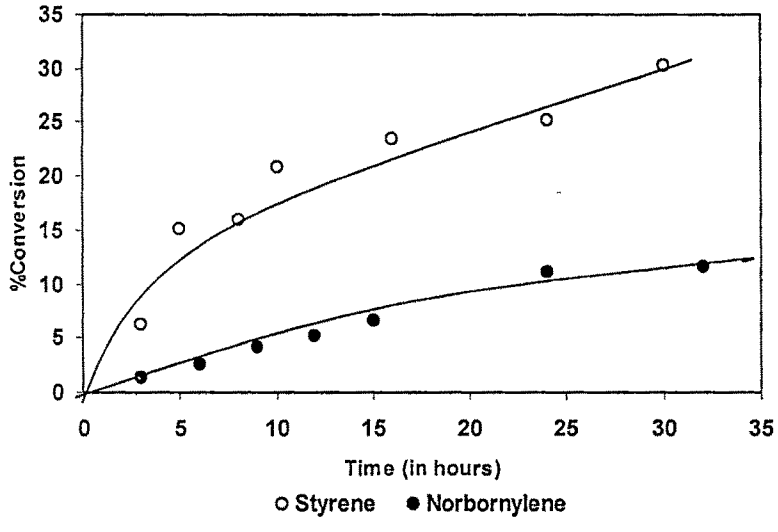

Fig. 3.1.6 Plot of conversion *vs* time for styrene and norbornylene using **Mn A**.

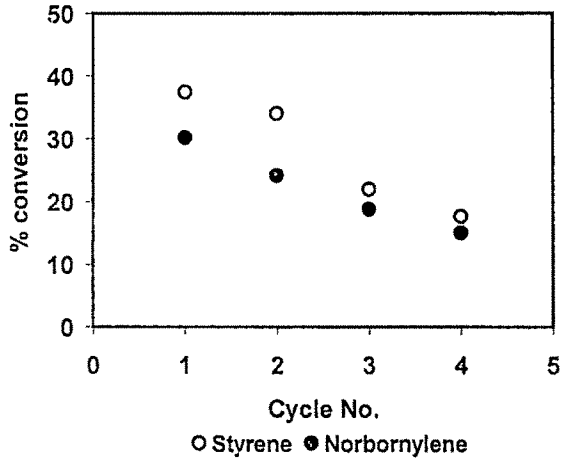

Fig. 3.1.7 Profile of catalyst recycle.

3.2. Poly(styrene-divinylbenzene) supported Ru(III) amino acid complexes

The following three ruthenium catalysts were prepared as per the sequence shown in **Scheme 3.2.1.**

Ru A = 8% Poly(S-DVB)L-val Ru(III) complex

Ru B = 6% Poly(S-DVB)L-val Ru(III) complex

Ru C = 8% Poly(S-DVB)L-ph ala Ru(III) complex

Complex formation

The reaction of hydrated ruthenium(III) chloride with polymer anchored amino acid was conducted in the pH range of 2.4 – 2.5. A maximum Ru loading of 1.7% / gm resin was obtained (**Table 3.2.1.**). For the trivalent Ru^{3+} ion, the formation of $[Ru(amino\ acid)_2Cl_2]Cl$ type of chelate may be favoured and the possible structure is depicted in **Scheme 3.2.1.**

Catalyst characterization

Some of the important physical properties of these catalysts have been measured and the data compiled in **Table 3.2.2.** **Ru B** has a slightly higher surface area and larger pore volume than **Ru A** & **Ru C**. The metal loading on **Ru A** & **Ru C** (Ru 1.7% & 1.65% /gm resin) were slightly higher than in **Ru B** (Ru 1.3% /gm resin) (**Table 3.2.1.**). The results of swelling behavior again indicate that swellability increased in polar solvents than in non-polar aliphatic and aromatic hydrocarbon solvents (**Table 3.2.3.**).

Representative IR spectra of polymer supports and catalysts are shown in **Fig. 3.2.1(a & b)**. As discussed in the previous section the amino acid coordinates to Ru through N(amino) and O(carboxylate) groups in the anchored complexes. Weak intensity bands in the far IR region at ~300-310 cm^{-1} and 440-460 cm^{-1} have been assigned to ν Ru-Cl and ν Ru-N/O vibrations [23,24].

The diffuse reflectance spectra (200-700 nm) of **Ru A** and **Ru B** exhibit two strong absorption bands at 350 nm and 400 nm respectively with reference to $BaSO_4$ standard (**Fig. 3.2.2**). These are assigned to $\pi \rightarrow t_{2g}$ charge transfer bands as has been observed for many mono-nuclear Ru(III) compounds [23-26]. No other spin allowed *d-d* transitions were observed in the visible region. Based on the structural feature of six coordinate complexes derived from $RuCl_3$ and bidentate ligands, for e.g. $[Ru(en)_2Cl_2]Cl$ (en = $NH_2(CH_2)_2NH_2$) or $[Ru(bipy)_2Cl_2]Cl$ (bipy = 2,2'-bipyridyl), it is possible to envisage similar octahedral stereochemistry for the present L-valine complexes represented as $[Poly(L\text{-}val)_2RuCl_2]Cl$ (**Scheme 3.2.1**). Conductance measurements in solution have been used for confirming the 1:1 electrolytic nature of homogeneous complexes [24]. However, as no simple and reliable measurement techniques are available to ascertain this property of metal complex on a rigid polymeric surface, the structure postulated for the present Ru(III) complexes shown in **Scheme 3.2.1** needs further confirmation. Complexes of Co(III) & Ru(III) with nitrogen ligands have been anchored to polyvinyl pyridine support to form compounds formulated as $[(PVP)\text{-}Co(en_2)Cl]Cl_2$ or $[(PVP)\text{-}Ru(bipy)_2Cl_2]Cl$ [27,28] which indirectly support the O_h geometry depicted in **Scheme 3.2.1** for our complexes.

Scanning electron micrographs (SEM) of ruthenium catalysts were recorded as described in the **section 3.1**. Comparison of images taken at a magnification of ~$3x10^3$ again showed that the smooth and flat surface of the starting poly (S-DVB) (**Fig. 3.2.3a**) is distinctly altered, exhibiting considerable roughening of the top layer upon anchoring of the amino acid (**Fig. 3.2.3b**). After metal incorporation, randomly oriented dark depositions on the external surface of the resin were seen (**Fig. 3.2.3c**).

The TG analysis showed that the polymer supported ruthenium catalysts degrade at considerably lower temperatures (**Table 3.2.4.**) than the unsupported polymer. The variation in cross-linking in these cases also, does not show much deviation in their thermal stabilities as found from the wt. loss (~21% at 350-370°C). Similarly, as in the case of Mn catalysts, a small weight loss (~2%) at ~110°C was also observed for the Ru catalysts. Representative TG are depicted in **Fig. 3.2.4.**

The X-band EPR spectrum of one of the catalyst **Ru A,** recorded in the solid state at room temperature displays broad signals as shown in **Fig. 3.2.5.** (spectrometer settings: micro wave frequency 9.5 MHz; microwave power 10.0 mw; modulation amplitude 2G; gain 1.25 x 10^4). The spectra can be interpreted assuming an axial symmetry for an isolated S = ½ low spin $(t_{2g})^5$ Ru(III) ion using the Spin-Hamiltonian suggested by Drago et. al [29]. The broadening of signals with increase in temperature is on account of the effects of large spin-orbit coupling constant (λ) for Ru(III). As the temperature is raised the orbital angular momentum on the metal probably couple with the electron spin leading to extremely short relaxation times accompanied by broad EPR lines. The spectrum of **Ru A** is characterized by two resonances in the $g_\perp$ region ($g_\perp = 2.91$) which are split into two components with the $g_{||}$ resonance observed at 2.26. No hyperfine

splitting is noticed at this temperature. Interestingly, the spectral features have been ascribed by some workers to the presence of mixed valent Ru (III)/(II) species for dimeric ruthenium complexes [23,29-31]. The ESR spectra of high- spin Ru^{+2} ($4d^6$) ion would be difficult to observe and is not consistent with the spectrum in this study. Similarly low spin Ru^{+2} ($4d^6$)ion would be ESR silent. Therefore, it seems unlikely that the observed spectral feature in our case can be due to the simultaneous existence of Ru in two different oxidation states on a rigid polymeric support.

Catalytic evaluation

Polymer bound Ru(III)-L-valine complexes **Ru A** & **Ru B** were examined as catalysts in the epoxidation of various olefinic substrates and oxidation of alkanes in the presence of TBHP as the terminal oxidant. (**Ru C** was evaluated in asymmetric epoxidation which is described in section 3.5). Blank experiments revealed that no reaction occurred in the absence of either the catalyst or the oxidant. The results of epoxidation/oxidation carried out at two different temperatures are compiled in **Table 3.2.5.** All substrates undergo epoxidation/oxidation in presence of the Ru supported catalysts and in some cases very high selectivities are obtained. As in the case of Mn-catalysts styrene epoxidation resulted in multiple product formation. Expectedly overall yields are higher at 45°C than at 28°C. Formation of benzaldehyde (sel. 67%) as the major product suggests that the reaction with hydroperoxide proceeds from an independent oxidative cleavage pathway [21]. Norbornylene and *cis*-cyclooctene selectively yield corresponding epoxides (yield = 42% & 13% respectively). In case of cyclohexene only traces of epoxide were detected. The overall yields however, are very

high (yield = 65%) and product of allylic oxidation were observed. Toluene oxidation results in selective formation of benzaldehyde whereas in case of cyclohexane both cyclohexanol and cyclohexanone were obtained (**Table 3.2.5.**).

In order to verify whether the catalysts operate in a truly heterogeneous manner, the probe suggested by Sheldon *et. al.* [20] was applied to our system. 'Hot filtration' test as described in section 3.1 indicated *heterogeneous* nature of the polymer supported Ru-amino acid complexes.

The influence of reaction condition on catalytic activity was studied using **Ru A**. The results are presented in **Table 3.2.6.** As can be inferred from the Table reaction at 45°C are much more facile than at 28°C at similar levels of catalyst concentrations. The reactivity pattern for different solvents follows the order $CH_3OH < CH_2Cl_2 < CH_3CN$. With regard to the nature of oxidants, it was found that only TBHP was effective in all runs. Practically no oxidation takes place with either molecular oxygen (at room temperature as well as under drastic conditions: 45°C, 200psi O_2, 6 h) or hydrogen peroxide.

In situ generated homogeneous complex of $RuCl_3$ and L-valine (reacted in 1:2 molar ratio) gave slightly higher yields (60.2% & 48.4%) for epoxidation of styrene and norbornylene respectively than for **Ru A** & **Ru B** (52.8% & 42.7%) under identical conditions.

A brief kinetic study on the epoxidation of styrene and norbornylene in presence of TBHP at 28°C was investigated up to about 30 h by analyzing aliquots of reaction mixture at regular intervals of time. In **Fig. 3.2.6** is shown a plot of olefin conversions *vs.*

reaction time under a fixed oxidant concentration. Reaction rates are apparently higher with styrene than with norbornylene.

Catalyst recycling

The purpose of heterogenizing a homogeneous metal complex by anchoring to a polymer support is to evaluate its potential for practical applications. The recycling efficiency of **Ru A** was examined using styrene and norbornylene as substrates. These results are shown in **Table 3.2.7.** It was found that the yields diminished with successive recycling step. Estimation of Ru present in the recycled catalyst after four cycles gave a value of 0.82% Ru indicating some leaching of metal from the support. However, the solution containing the leached metal is inactive for catalysis as was confirmed by the 'hot filtration' test described in the earlier section. The activity profile for four successive cycles is depicted in **Fig. 3.2.7**. Comparison of DRS of recycled catalyst with the fresh **Ru A** (**Fig. 3.2.8**) revealed the absence of charge transfer band at 375 nm while a single peak at ~ 350 nm was observed. No new band due to high valent Ru could be seen in the region. Generally, $Ru^{VI} = O$ species (recognized as the active intermediates in catalytic oxidations) have been identified by characteristic absorptions in the visible region typically between 500-600 nm [32]. However, it was not possible to ascertain the nature of active species on the surface of the support from the observed spectral feature of recycled catalyst **Ru A**.

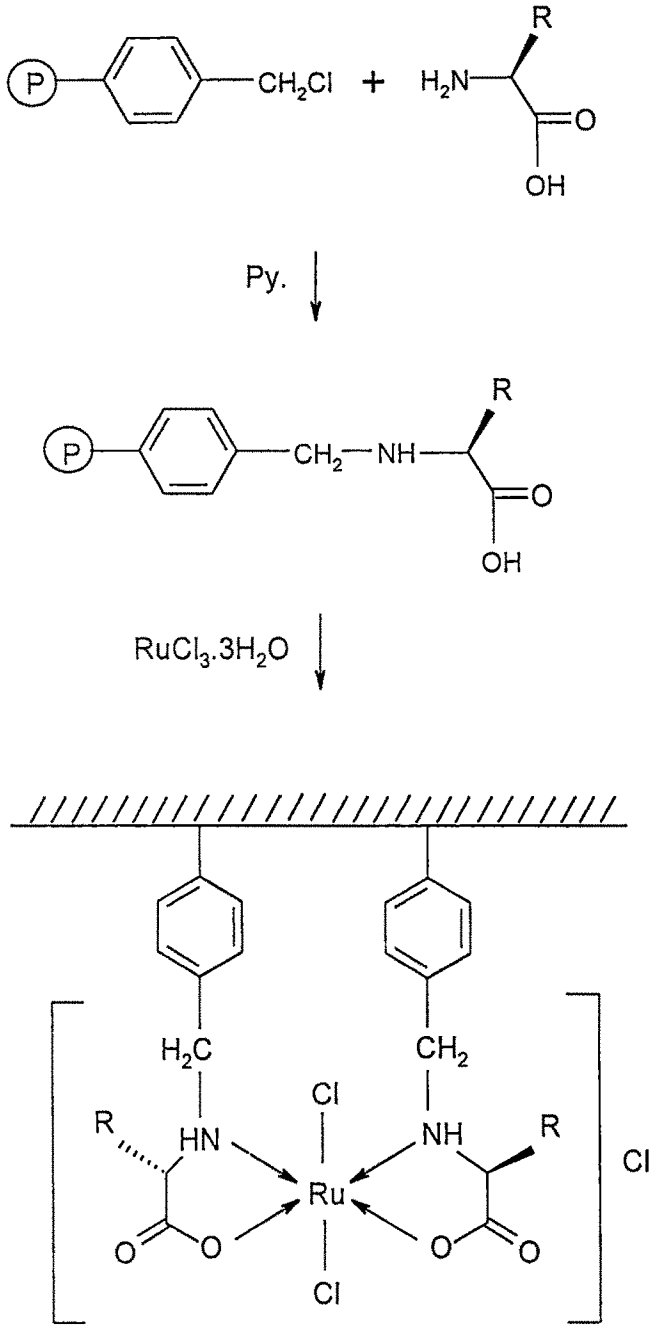

R = -$CH(CH_3)_2$ for L-val ; R = -CH_2Ph for L-ph ala

Scheme 3.2.1. Synthesis of poly(S-DVB) supported amino acid Ru(III) complex.

Table 3.2.1. Analytical data of Polymer Support, Ligand and Ru-anchored catalysts

Compound	C%	H%	Cl%	N%	Ru%
8%Poly(S-DVB)CH_2Cl	70.38	5.77	17.56	--	--
6%Poly(S-DVB)CH_2Cl	76.26	6.36	16.14	--	--
8%Poly(S-DVB)-Lval	60.15	5.00	9.47	2.56	--
6%Poly(S-DVB)-Lval	63.28	5.44	9.48	2.47	--
8%Poly(S-DVB)-L-ph ala	62.19	5.59	9.82	2.34	--
Ru A	57.23	4.79	n.d.	2.61	1.71
Ru B	59.90	5.23	n.d.	2.70	1.30
Ru C	59.83	5.42	n.d.	2.33	1.65

n.d. = not determined

Table 3.2.2. Physical properties of Ru-supported Poly(S-DVB) catalysts

Sample	Surface Area ($m^2 g^{-1}$)	Bulk Density ($g\ cm^{-3}$)	Pore volume ($cm^3 g^{-1}$)
8%Poly(S-DVB)CH_2Cl	32.7	0.44	0.20
6%Poly(S-DVB)CH_2Cl	38.3	0.38	0.29
Ru A	23.5	0.51	0.14
Ru B	36.9	0.46	0.18
Ru C	27.8	0.52	0.16

Table 3.2.3. Swelling data of Ru A, Ru B and Ru C in different solvents (mol %)

Solvent	8% Poly (S-DVB)CH_2Cl	8% Poly (S-DVB)CH_2Cl	**Ru A**	**Ru B**	**Ru C**
Acetonitrile	1.9	2.0	1.6	1.6	1.6
Benzene	1.1	1.1	0.8	0.9	0.9
Dichloromethane	1.5	1.8	1.3	1.3	1.2
Ethanol	1.7	1.9	1.6	1.6	1.5
n-Heptane	0.6	0.6	0.5	0.6	0.5
Methanol	2.7	2.8	2.2	2.3	2.3
Tetrahydrofuran	1.4	1.5	1.0	0.9	0.9
Toluene	1.1	1.1	0.8	0.8	0.7

Table 3.2.4. TG data of polymeric supports and anchored Ru(III) catalysts

Compound	Degr. Temp.(°C)	Wt. loss (%)
8%Poly(S-DVB)CH_2Cl	440	21.0
6%Poly(S-DVB)CH_2Cl	410	21.0
Ru A	111	2.4
	370	21.2
Ru B	110	2.0
	350	21.0
Ru C	106	2.0
	368	21.8

Table 3.2.5. Catalytic oxidation with Ru A and Ru B

Catalyst[a]	Substrate[b]	Temp. (°C)	Yield (%)[c]	Products/ Selectivity (wt. %)				TON[d]
				Epoxide	PhCHO	PhCOMe		
Ru A		28	40.4	21.2	67.2	11.0		80
Ru A	Styrene	45	52.8	37.5	49.3	13.2		105
Ru B		28	41.8	14.7	70.1	14.7		109
Ru B		45	53.8	23.8	57.5	18.7		141
Ru A		28	30.7	100.0				61
Ru A	Norbornylene	45	42.7	100.0				84
Ru B		28	24.4	100.0				65
Ru B		45	40.0	100.0				106
Ru A		28	6.0	100.0				13
Ru A	*cis*-cyclooctene	45	7.8	100.0				16
Ru B		45	13.0	100.0				34
				Epoxide	1-one	1-ol	Cy-one	
Ru A		28	38.1	Trace	36.0	31.5	32.0	78
Ru A	Cyclohexene	45	53.9	Trace	22.8	26.4	50.8	111
Ru B		45	65.2	2.55	36.9	25.4	35.1	169
					PhCHO			
Ru A		28	7.1		100.0			4
Ru A	Toluene[e]	45	10.3		100.0			6
Ru B		28	6.8		100.0			5
Ru B		45	10.1		100.0			8
				Cy-one	Cy-ol	Cy-ol/Cy-one		
Ru A		28	18.2	79.6	20.5	0.26		11
Ru A	Cyclohexane[e]	45	29.3	70.7	29.3	0.40		17
Ru B		28	17.8	85.6	14.4	0.20		14
Ru B		45	29.0	71.7	28.3	0.38		23

a = 0.15 g ; b = 5.0 mmol ; c = yield based on starting material ; d =Turnover number = mmol products/mmol Ru ; 1-one = cyclohexene-1-one ; 1-ol = cyclohexene-1-ol ; Cy-one = cyclohexanone; e = (0.2 g cat. & 2.0 mmol substrate), solvent = acetonitrile.

Table 3.2.6. Epoxidation of styrene & norbornylene by Ru A under different reaction conditions

	Catalyst wt. (g)	Temp. (°C)	Solvent[c]	Oxidant	TON[d]
	0.15	45	CH_3CN	TBHP	65 (38)
Temp.[a]	0.15	28	CH_3CN	TBHP	41 (26)
	0.15	8-10	CH_3CN	TBHP	18 (21)
	0.10	45	CH_3CN	TBHP	110 (83)
Catalyst conc.[b]	0.15	45	CH_3CN	TBHP	105 (84)
	0.20	45	CH_3CN	TBHP	100 (74)
	0.15	28	CH_3CN	TBHP	80 (65)
Solvent[b]	0.15	28	CH_2Cl_2	TBHP	53 (62)
	0.15	28	CH_3OH	TBHP	31 (8)
	0.15	28	CH_3CN	H_2O_2	03 (0)
Oxidant[b]	0.15	28	CH_3CN	O_2	0.5 (0)
	0.15	28	CH_3CN	CHP	18 (164)

a = reaction time = 8 h; b = reaction time = 24 h; c = 20ml; d = values in parentheses are for norbornylene; substrate conc. = 5.0 mmol.

Table 3.2.7. Recycling study of Ru A[a]

Cycle no.	Yield (%)[b]	
	styrene	norbornylene
1	49.4	40.5
2	38.0	32.2
3	26.6	23.5
4	18.8	19.4

[a] Conditions: 150 mg cat.; 5.0mmol olefin; 10.0 mmol TBHP; 20 ml CH_3CN; 45°C; 24 h.
[b] Yield based on starting material.

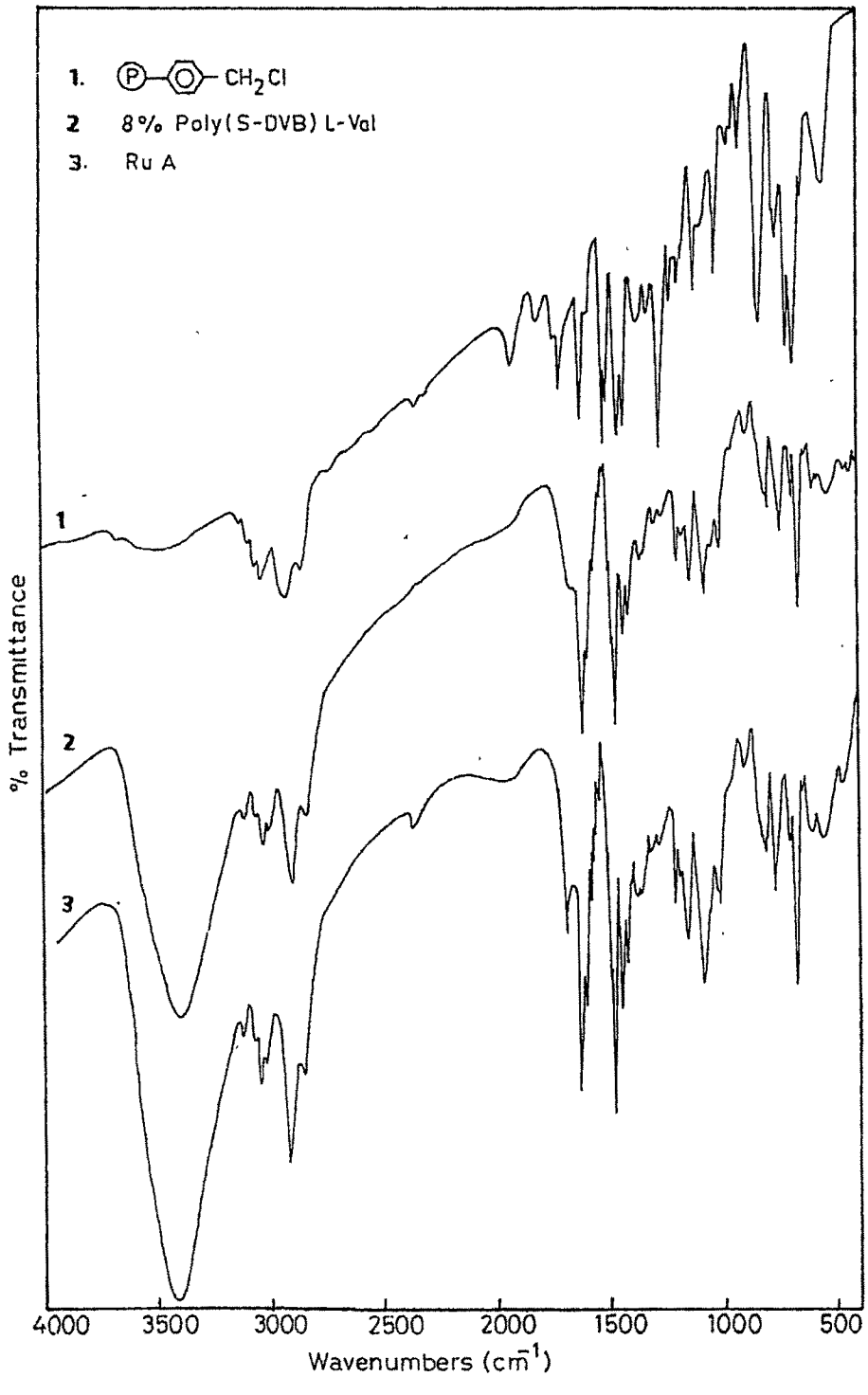

Fig. 3.2.1(a) FT-IR spectra of support, liganded polymer and catalyst.

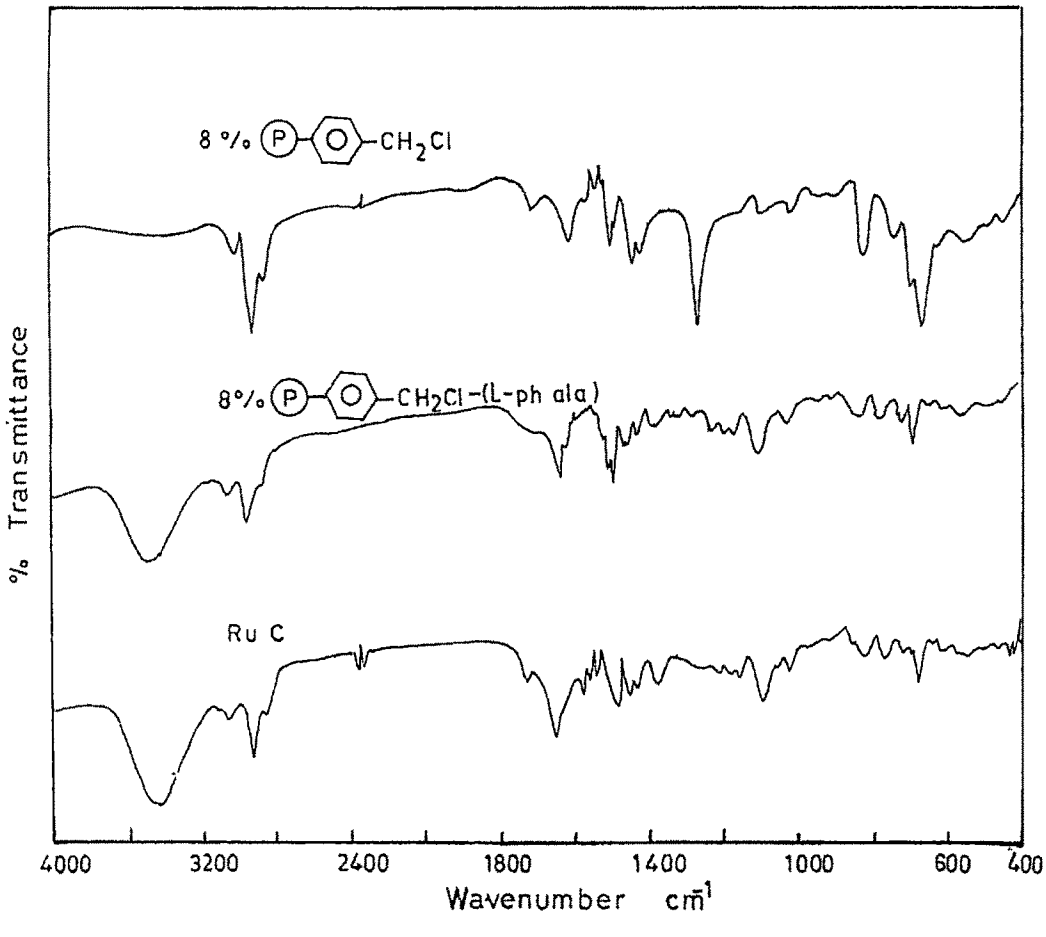

Fig. 3.2.1(b) FT-IR spectra of support, liganded polymer and catalyst.

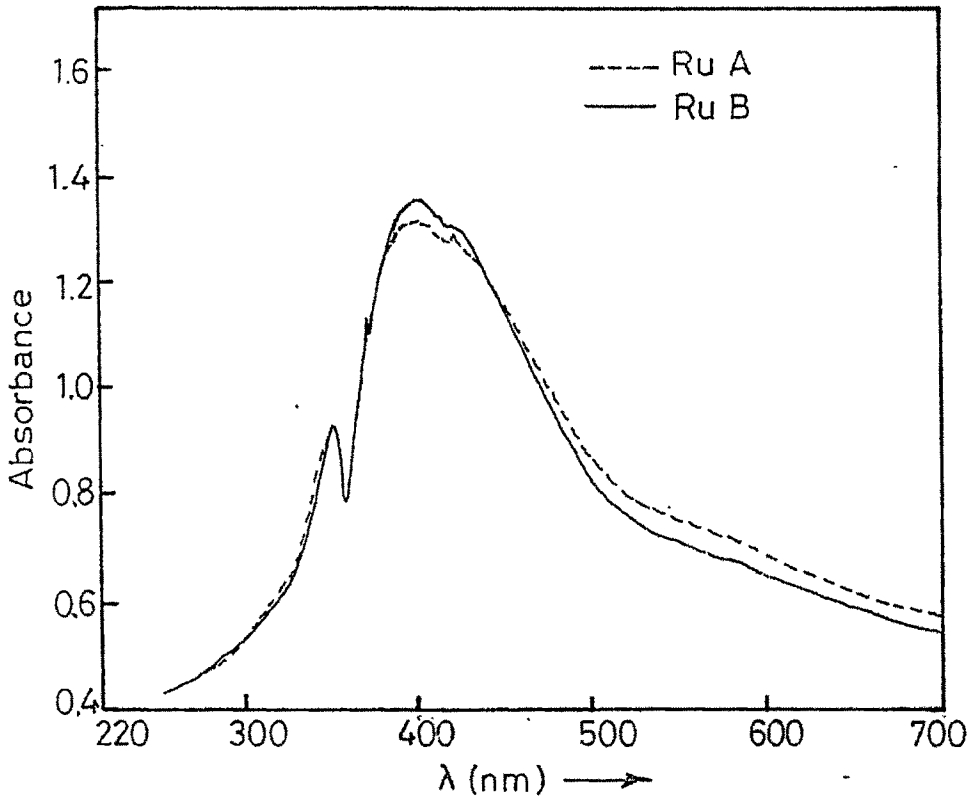

Fig. 3.2.2 Diffuse reflectance spectra of catalysts

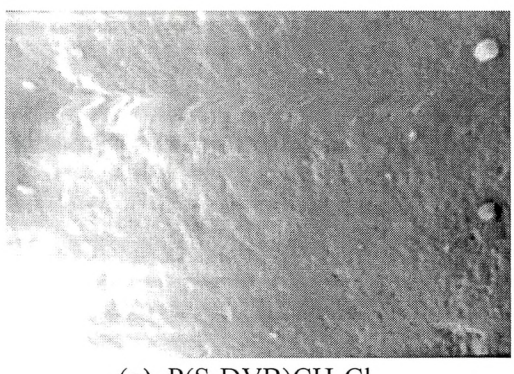

(**a**) P(S-DVB)CH_2Cl

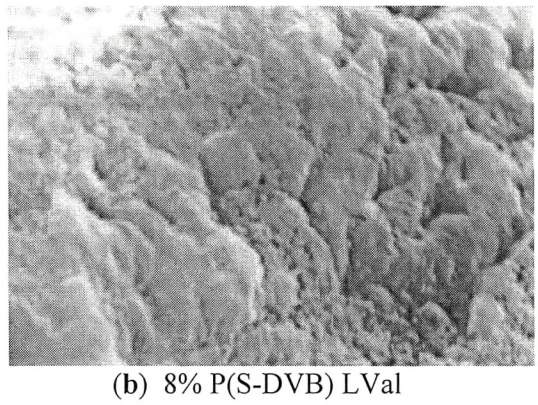

(**b**) 8% P(S-DVB) LVal

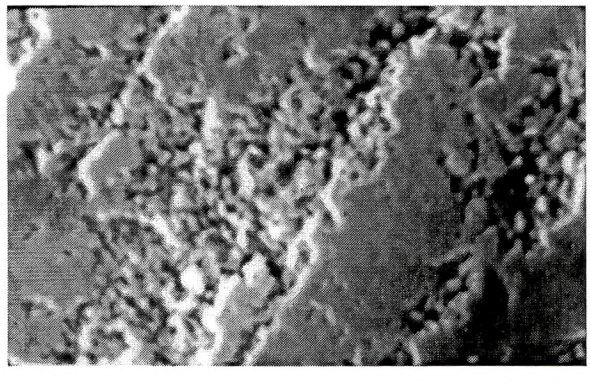

(**c**) Ru **A**

Fig. 3.2.3 Scanning electron micrographs

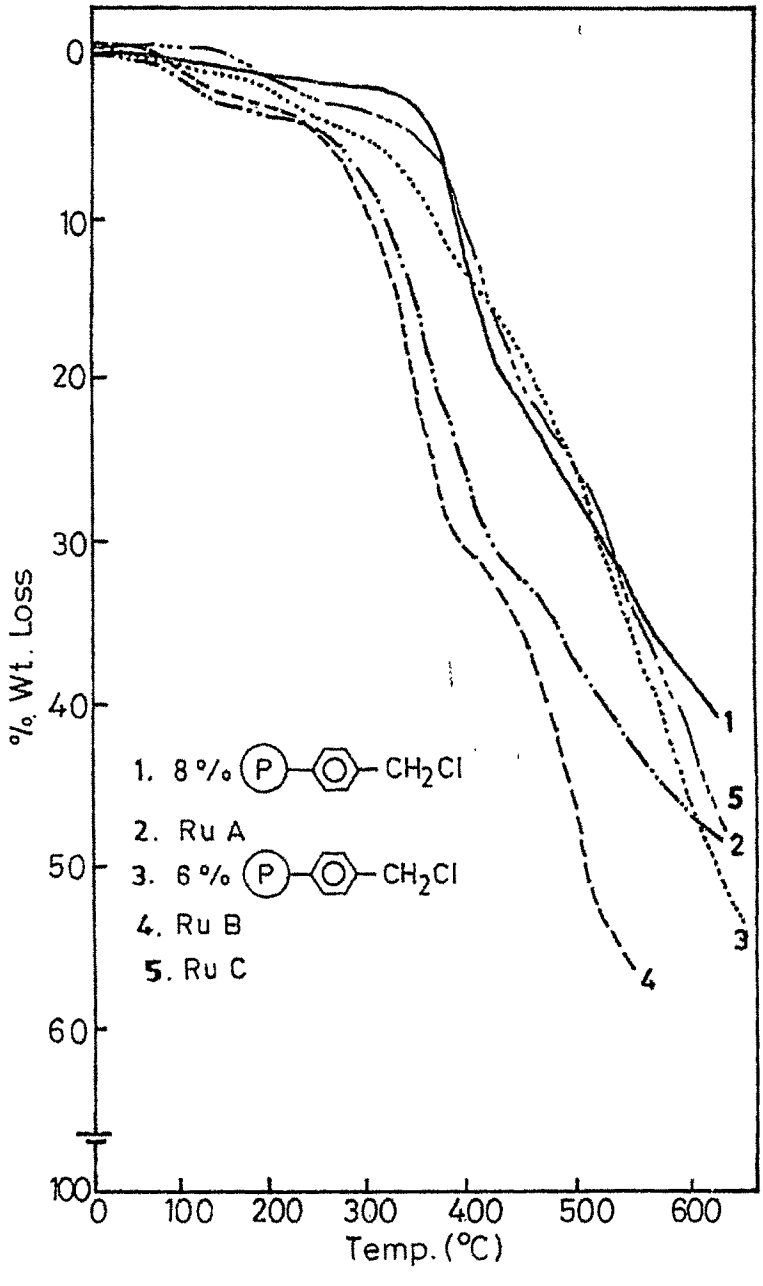

Fig. 3.2.4 TG of support and Ru catalysts.

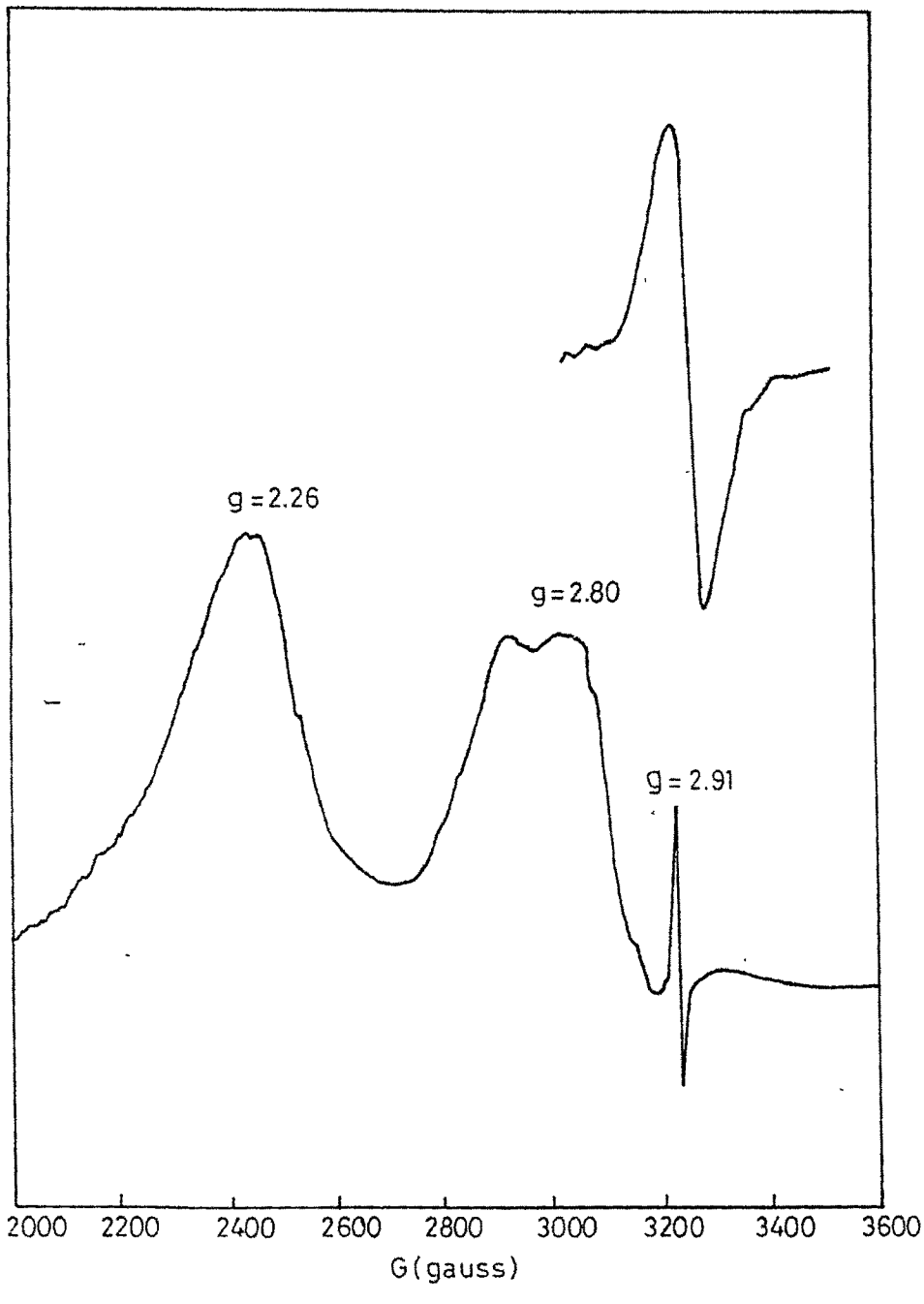

Fig. 3.2.5 ESR spectra of **Ru A**

Inset: resonance signal with field set at 3.2 kG, Scan range 400G, gain 1.25 x 10^4.

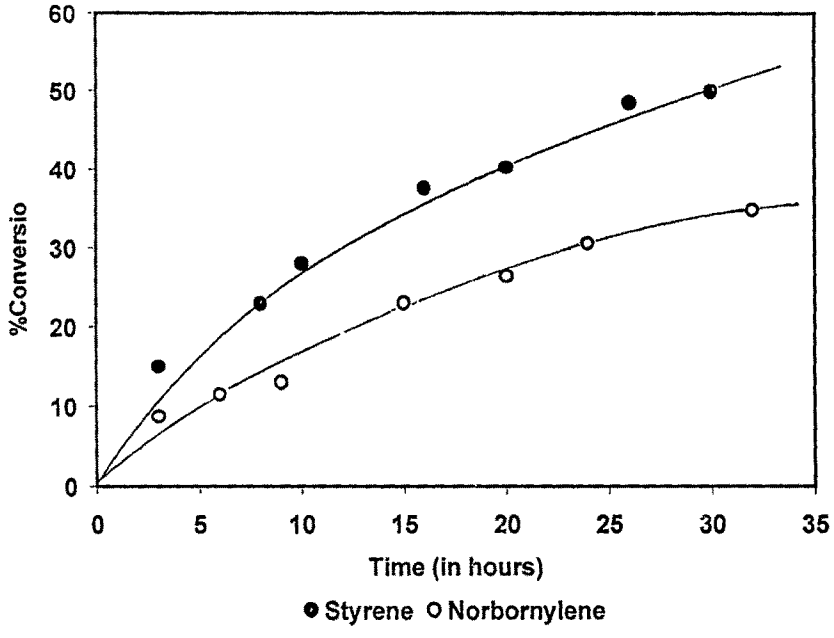

Fig. 3.2.6 Plot of conversion *vs* time for styrene and norbornylene using **Ru A**.

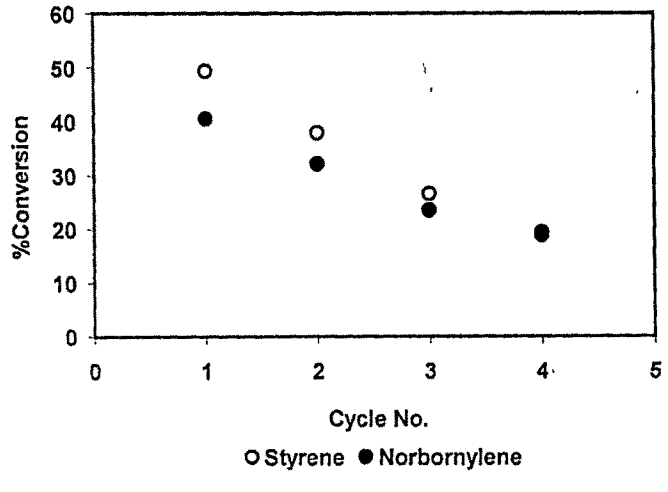

Fig.3.2.7 Profile of catalyst recycle.

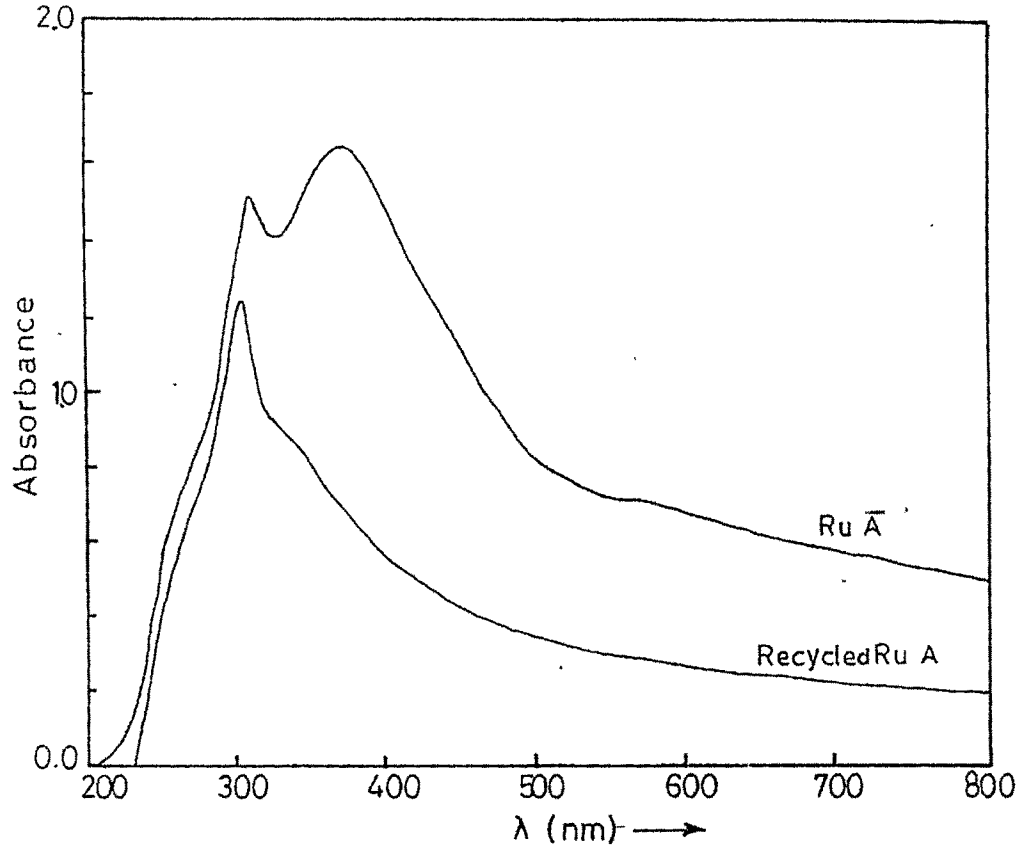

Fig. 3.2.8 Diffuse reflectance spectra of recycled **Ru A.**

3.3. Poly(styrene-divinylbenzene) supported Cu(II) amino acid complexes

The copper catalysts studied in this section are designated as under:

Cu A = 8% Poly(S-DVB)L-val Cu(II) complex

Cu B = 6% Poly(S-DVB)L-val Cu(II) complex

Cu C = 8% Poly(S-DVB)L-ph ala Cu(II) complex

Complex formation

Reaction of copper acetate with polymer anchored amino acid was conducted in the pH range of 3.5 – 3.6. A maximum Cu loading of up to 3.59% /gm resin was obtained (**Table 3.3.1.**). For the bivalent Cu^{2+} ion, the formation of [Cu(amino acid)$_2$] or [Cu(amino acid)$_2$(OAc)$_2$] type of chelate can be expected. The probable structure of complex is shown in **Scheme 3.3.1**.

Characterization of supported catalysts

Some of the key physical properties of Cu catalysts have been compiled in **Table 3.3.2.** **Cu B** has a slightly higher surface area and larger pore volume than **Cu A** & **Cu C**. The metal loading on **Cu A** & **Cu C** with 8% cross-link (Cu 3.50% & 3.10% / gm resin) was marginally lower than in **Cu B** with 6% cross-link (Cu 3.59% / gm resin) (**Table 3.3.1.**). There is a noticeable decrease in surface area of the supports by 19-33% after metal loading indicating possible blocking of pores on the external surface of polymer after complexation. Similar results have been reported for other surface modified

polymeric catalysts [33,34]. The results of swelling behavior indicate that swellability increased in polar solvents than in non-polar aliphatic and aromatic hydrocarbon solvents. All supported Cu catalysts showed lower swelling in polar as well as non polar solvents compared to the support (**Table 3.3.3.**).

Representative IR spectra of polymer supports and catalysts are shown in **Fig. 3.3.1**. Weak bands in the far IR region (~ 410 - 350cm^{-1}) can. be assigned to ν Cu-N and ν Cu-O vibrations [35]. The location of different peaks and the corresponding shifts follow similar trend as described earlier for Mn & Ru catalysts.

The diffuse reflectance spectra (200-800 nm) of **Cu A** and **Cu B** display nearly identical features with two strong absorption bands in the uv region at ~310 nm and ~370 nm (ligand to metal charge transfer bands) and very weak & broad band in the visible region at 570 nm with reference to the $BaSO_4$ standard (**Fig. 3.3.2**). Absorption spectrum of Cu-proteins show characteristic LMCT bands in the region of 250 nm and a relatively broad band around 620 nm [36,37]. These values are consistent with a N_2O_2 co-ordination (square planar) environment around the central Cu^{2+} ion. The possibility of octahedral co-ordination though remote, can be visualized by assuming monodentate co-ordination of acetate ions to yield [Cu(amino acid)$_2$(OAc)$_2$] type complex. The current evidence, however, appears to favour a predominantly *planar* configuration. Both these structural possibilities (I & II) are illustrated in **Scheme 3.3.1**.

The morphological changes occurring on the surface of catalyst before and after anchoring are evident as indicated by their scanning electron micrographs (**Fig. 3.3.3a – 3.3.3c**). After metal incorporation the complex appears to be irregularly dispersed along

the external surface of the resin.

The TG data for **Cu A** and **Cu B** are summarized in **Table 3.3.4.** and representative thermograms reproduced in **Fig. 3.3.4.** Similar conclusion regarding the thermal stability of **Cu A** & **Cu B** can be drawn as discussed in the earlier section for Mn Ru catalysts.

The X-band EPR spectrum of one of the catalyst **Cu A** recorded in the solid state at 297°K temperature showed signals characteristic of axial symmetry. Due to the irregular feature of resonance lines (**Fig. 3.3.5**) $A_{\parallel}$ value was computed by averaging over all 3 lines and is equal to ~167 G. The experimentally calculated $^{g}_{\perp}$ and $^{g}_{\parallel}$ values correspond to 2.10 and 2.31 which are of the same order as found in mononuclear Cu^{2+} amino acid complexes [36,38].

Catalytic evaluation

The results of oxidation carried out with **Cu A** and **Cu B** are compiled in **Table 3.3.5.** The substrates employed in oxidation reactions were styrene, benzyl alcohol and cyclohexanol. High selectivity were generally noted in case of alcohols. The 'hot filtration test ' [20] (45°C) showed a residual activity of ~2.9% for the *filtrate* after 24 h where as the *original* catalyst gave an overall conversion of 70% after the same period clearly indicating that the Cu-catalyst behave in a truly *heterogeneous* manner. Though our results showed minor leaching of Cu into the solution, the metal species leached into the filtrate are *inactive* and are *not responsible* for the observed catalytic activity.

Formation of benzaldehyde (sel. ~56%) as the major product during styrene epoxidation again suggests that the reaction with TBHP leads to oxidative cleavage of styrene[21]. Benzylalcohol and cyclohexanol are selectively converted to the corresponding aldehyde and ketone with both **Cu A & Cu B.** Weckhuysen et.al [36] reported that oxidation of benzyl alcohol with Cu(amino acid)$_2$ loaded on Zeolite support yield benzoic acid *in addition* to PhCHO in roughly 1:2 ratio. In our case the overall mass balance based on GC data indicate that >94% of the converted product corresponds to PhCHO. This difference in reactivity is attributed to the dissimilar nature of the supports employed for anchoring of Cu(II)-amino acid complexes as also to the predominantly acidic character of Zeolite structure. In all the examples discussed above **Cu A** displayed better activity compared to **Cu B.** A detailed study was undertaken with these two catalysts to understand the influence of reaction conditions on the oxidation of benzyl alcohol as a model substrate. The extent of oxidation observed at different temperatures and catalyst concentrations are presented in **Tables 3.3.5. - 3.3.6.** As can be inferred from the Table, increase in reaction temperature is accompanied by a marked improvement in yields at similar levels of catalyst concentrations. For instance, raising the reaction temperature from ambient (28°C) to 45°C results in more than two fold increase in yields with all substrates. Amongst the different solvents studied activity is maximum for acetonitrile followed by methylene chloride and methanol. With regard to the oxidants both TBHP and CHP were effective but low activity was observed with molecular oxygen or hydrogen peroxide.

A comparative oxidation test with *homogeneous* catalyst (generated in solution by mixing Cu(II) salt & L-valine in 1:2 mole

ratio) was carried out with benzyl alcohol in presence of TBHP under identical condition. The overall yields were generally lower (24.4%) than for the supported catalysts (**Table 3.3.5.**). Interestingly, nearly similar yields (26.2%) were observed when 1:1 (Cu : L-valine) homogeneous complex was employed in the reaction.

The UV-Vis solution spectra of both 1:1 and 1:2 *in situ* generated homogeneous Cu-L-valine complexes are blue in colour and exhibit a single *d-d* absorption band in the visible region at ~735 nm (**Fig 3.3.6**). The spectral features are distinctly different compared to the DRS of the polymer supported catalysts **Cu A** and **Cu B**. LMCT bands are not observed in the spectra of the homogeneous catalysts.

A preliminary kinetic study on the oxidation of benzyl alcohol in presence of TBHP at 28°C was investigated with **Cu A** and **Cu B** up to 24 h by analyzing aliquots of reaction mixture at regular intervals of time. In **Fig. 3.3.7** is shown a plot of alcohol conversion *vs.* reaction time under a fixed oxidant concentration. With both the catalysts the conversions increase almost linearly up to about 16 h but slows down thereafter.

Catalyst recycling

The recycling efficiency of **Cu A** and **Cu B** in the oxidation of benzyl alcohol was investigated. These results are compiled in **Table 3.3.7.** The catalyst was recycled four times without noticeable loss in activity. This trend is shown in **Fig. 3.3.8.** The DRS of recycled catalysts after the *first* cycle (**Cu A-1**) and *fourth* cycle (**Cu A-4**) were similar (**Fig 3.3.2**).

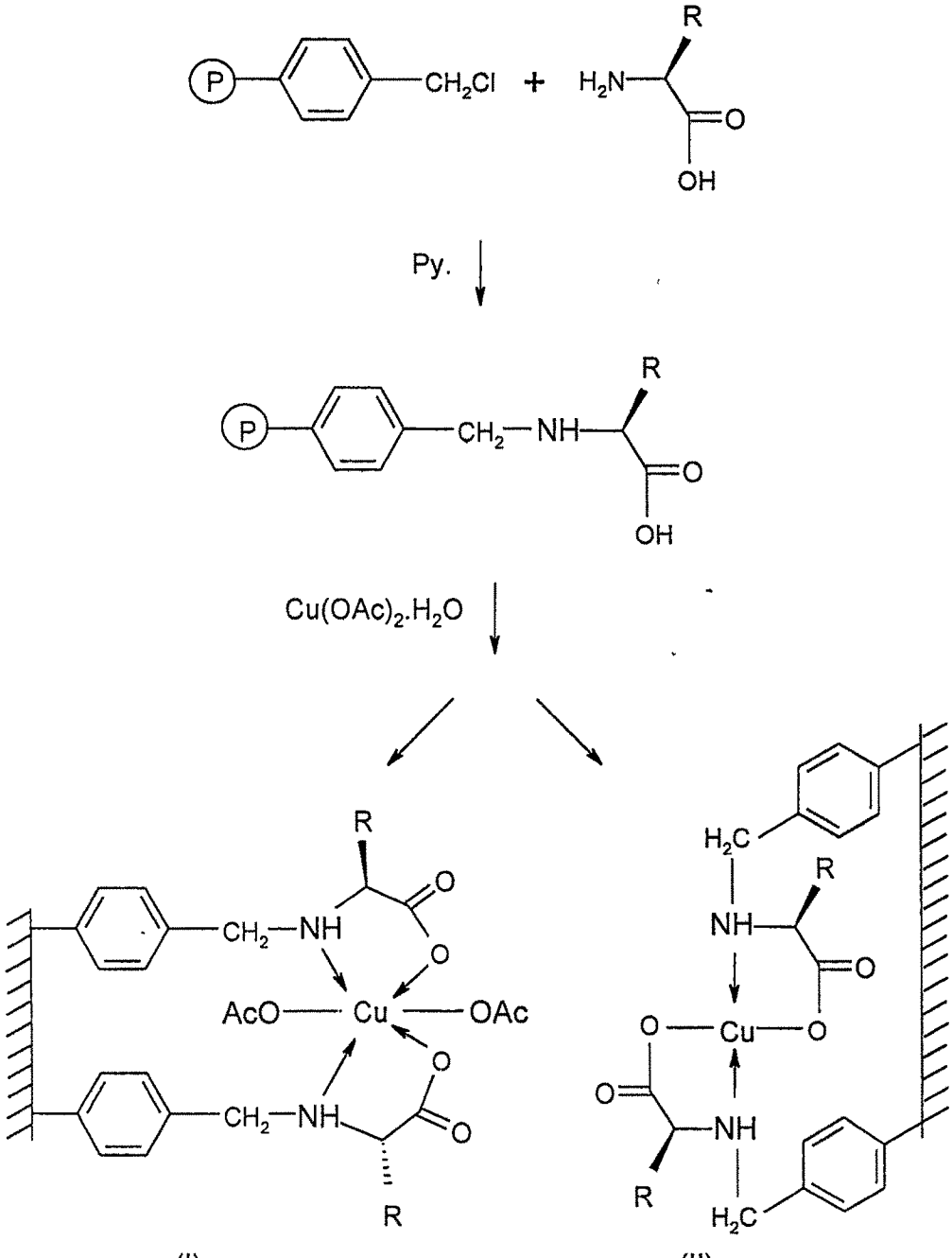

(I) (II)

R = -$CH(CH_3)_2$ for L-val.; R = -CH_2Ph for L-ph ala

Scheme 3.3.1. Synthesis of poly(S-DVB) supported amino acid Cu(II) complex.

Table 3.3.1. Analytical data of Polymer Support, Ligand and Cu-anchored catalysts

Compound	C%	H%	Cl%	N%	Cu%
8%Poly(S-DVB)CH_2Cl	70.38	5.77	17.56	--	--
6%Poly(S-DVB)CH_2Cl	76.26	6.36	16.14	--	--
8%Poly(S-DVB)-L-val	60.15	5.00	9.47	2.56	--
6%Poly(S-DVB)-L-val	63.28	5.44	9.48	2.47	--
8%Poly(S-DVB)-L-ph ala	62.19	5.59	9.82	2.34	--
Cu A	58.46	5.06	n.d.	2.46	3.50
Cu B	60.48	5.16	n.d.	2.41	3.59
Cu C	61.22	5.93	n.d.	2.37	3.10

n.d. = not determined

Table 3.3.2. Physical properties of Poly(S-DVB) supported Cu catalysts

Sample	Surface Area ($m^2 g^{-1}$)	Bulk Density ($g\ cm^{-3}$)	Pore volume ($cm^3 g^{-1}$)
8%Poly(S-DVB)CH_2Cl	32.7	0.44	0.20
6%Poly(S-DVB)CH_2Cl	38.3	0.38	0.29
Cu A	21.6	0.51	0.16
Cu B	30.6	0.45	0.19
Cu C	28.1	0.50	0.17

Table 3.3.3. Swelling study (mol %)

Solvent	8% Poly (S-DVB)CH_2Cl	6% Poly (S-DVB)CH_2Cl	**Cu A**	**Cu B**	**Cu C**
Acetonitrile	1.9	2.0	1.4	1.5	1.5
Benzene	1.1	1.1	0.8	0.8	0.8
Dichloromethane	1.5	1.8	1.2	1.4	1.2
Ethanol	1.7	1.9	1.5	1.6	1.7
n-Heptane	0.6	0.6	0.4	0.5	0.5
Methanol	2.7	2.8	2.2	2.5	2.2
Tetrahydrofuran	1.4	1.5	1.0	1.0	0.9
Toluene	1.1	1.1	0.8	0.9	0.8

Table 3.3.4. TG data of polymeric supports and anchored Cu(II) catalysts

Compound	Degr. Temp.(°C)	Wt. loss (%)
8%Poly(S-DVB)CH_2Cl	440	21.0
6%Poly(S-DVB)CH_2Cl	410	21.0
Cu A	111	2.2
	370	23.0
Cu B	112	1.8
	372	20.0
Cu C	108	2.1
	366	20.8

Table 3.3.5. Catalytic oxidation with Cu A and Cu B

Catalyst[a]	Substrate[b]	Temp. (°C)	Yield (%)[c]	Products/ Selectivity (wt. %)		
				epoxide	PhCHO	PhCOMe
Cu A		28	28.6	9.6	81.1	9.3
Cu A	Styrene	45	60.6	22.8	56.4	20.8
Cu B		28	19.2	16.0	56.4	27.1
Cu B		45	51.2	20.5	56.2	23.2
Cu A		28	30.8		94.7	
Cu A	Benzyl alcohol	45	72.0		93.8	
Cu B		28	30.0		94.4	
Cu B		45	70.0		93.6	
				cyclohexanone		
Cu A		28	12.8	100.0		
Cu A	Cyclohexanol	45	24.6	100.0		
Cu B		28	11.2	100.0		
Cu B		45	25.4	100.0		

a = 0.10 g ; b = 5.0 mmol ; c = yield based on starting material.

Table 3.3.6. Oxidation of benzyl alcohol using Cu A & Cu B under different reaction conditions.

Parameter	Catalyst wt. (g)	Oxidant	Solvent	Yield (%)[a]
	0.05	TBHP	CH_3CN	22.0 (22.4)[b]
Catalyst conc.	0.10	TBHP	CH_3CN	30.8 (30.0)
	0.15	TBHP	CH_3CN	38.8 (39.6)
	0.10	TBHP	CH_3CN	30.8 (30.0)
Oxidant	0.10	H_2O_2	CH_3CN	10.8 (5.8)
	0.10	O_2 gas[c]	CH_3CN	6.8 (6.4)
	0.10	CHP	CH_3CN	37.0 (37.6)
	0.10	TBHP	CH_3CN	30.8 (30.0)
Solvent	0.10	TBHP	CH_2Cl_2	18.8 (19.6)
	0.10	TBHP	CH_3OH	15.6 (9.4)

Temp. 28°C; 24 h; a = yield based on starting material; b = values in parentheses are for **Cu B** ; c = 200psi O_2; Substrate = 5.0 mmol.

Table 3.3.7. Catalyst recycling in the oxidation of benzyl alcohol using TBHP[a]

Cycle no.	Yield (%)[b] Cu A	Cu B
1	71.6	70.4
2	66.8	65.3
3	62.6	62.0
4	60.7	60.2

a = Reaction conditions: 100 mg catalyst; 7.5 mmol TBHP; solvent = acetonitrile (20 ml); 45°C; 24 h; substrate=5.0 mmol; b = Yield based on starting benzyl alcohol.

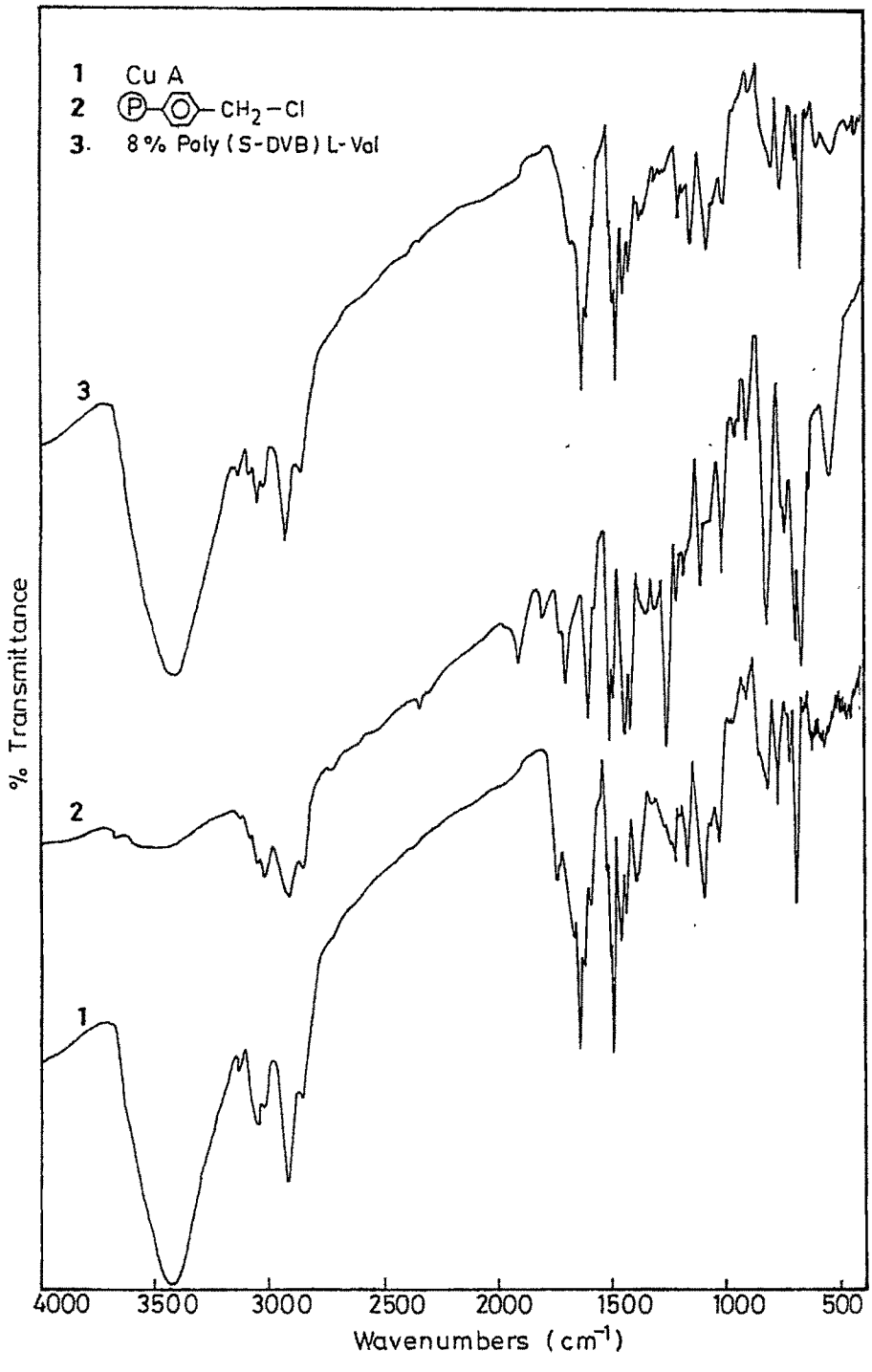

Fig. 3.3.1 FT-IR spectra of support, liganded polymer and catalyst

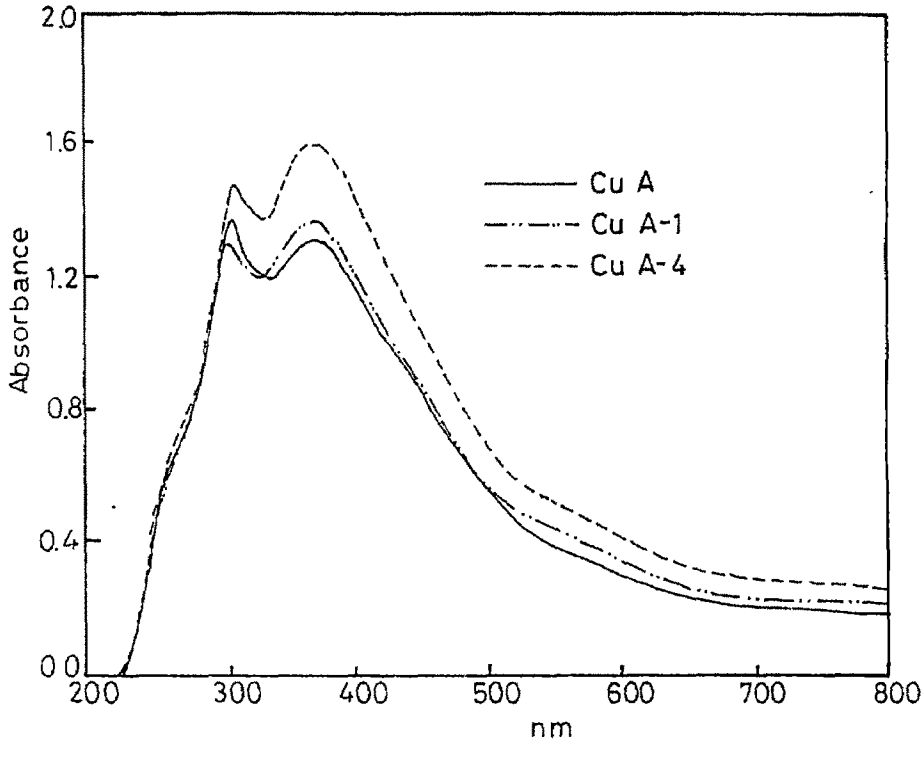

Fig. 3.3.2 Diffuse reflectance spectra of catalysts

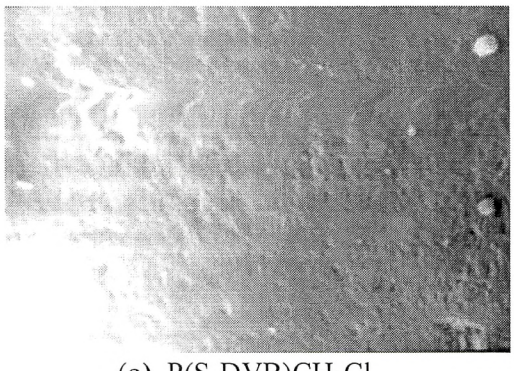

(**a**) P(S-DVB)CH_2Cl

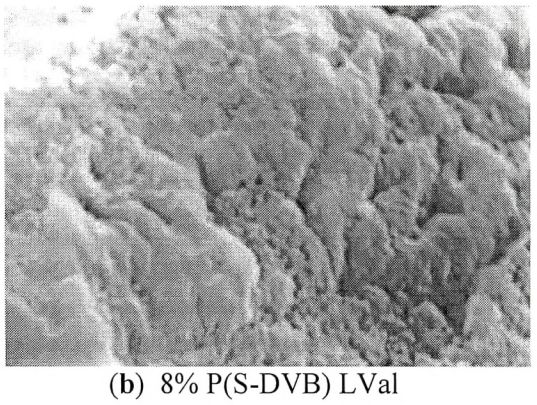

(**b**) 8% P(S-DVB) LVal

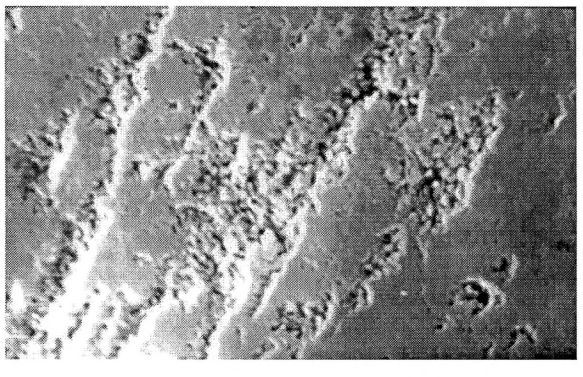

(**c**) Cu **A**

Fig. 3.3.3 Scanning electron micrographs

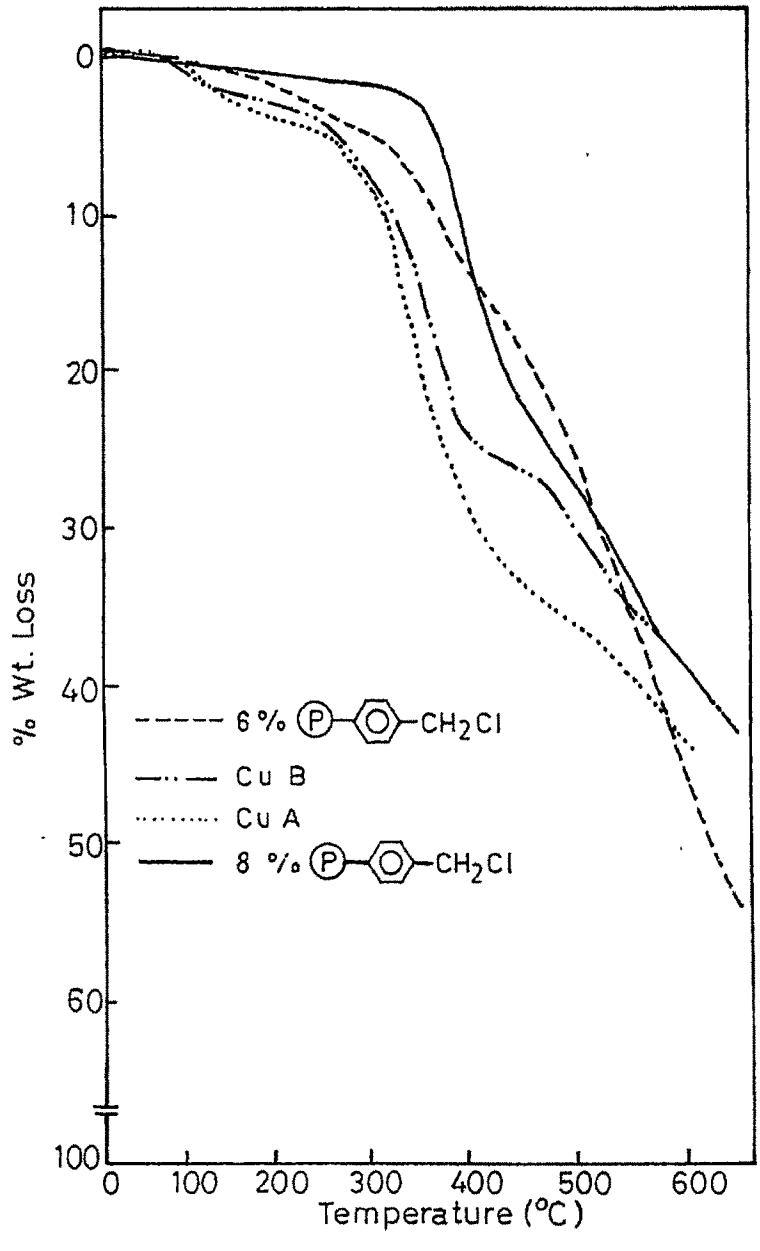

Fig. 3.3.4 TG of supports and catalysts.

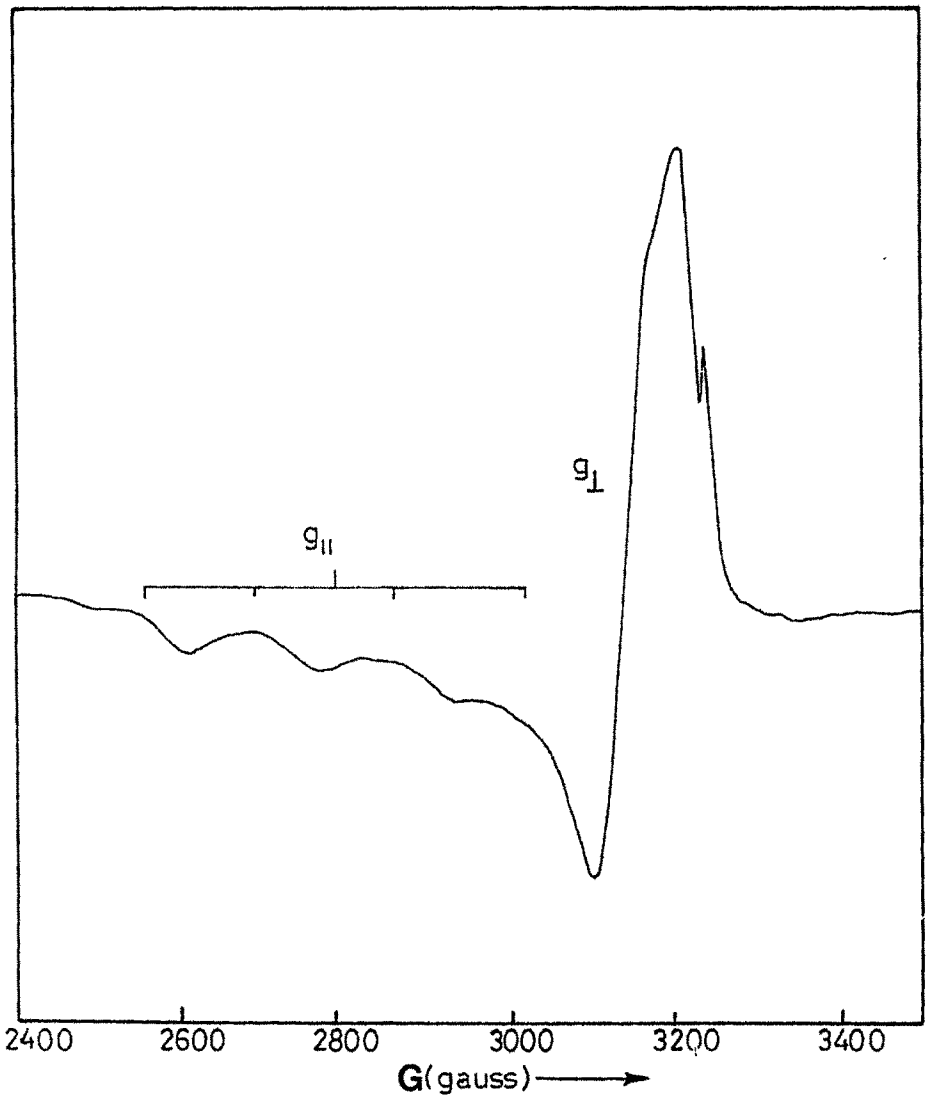

Fig. 3.3.5 ESR spectra of **Cu A.**

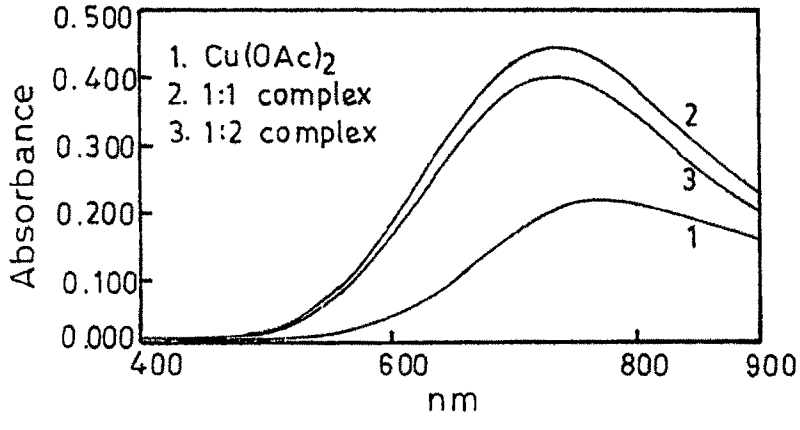

Fig. 3.3.6 UV-Vis solution spectra of homogeneous complexes

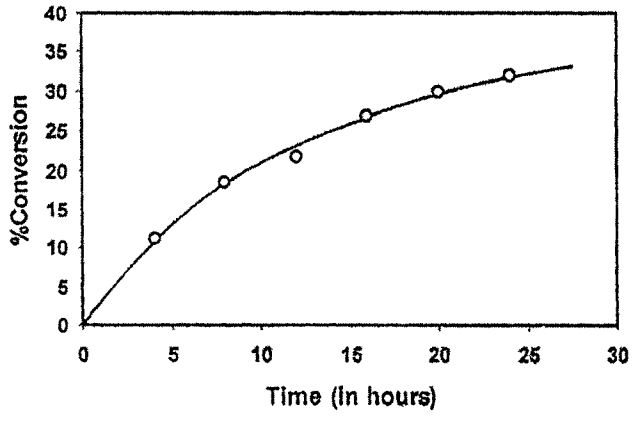

(a)

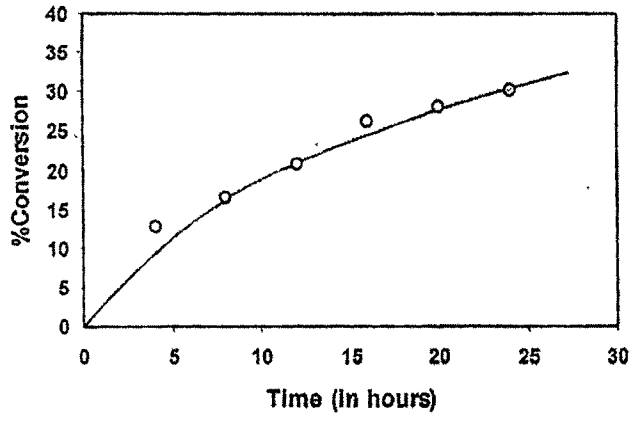

(b)

Fig. 3.3.7 Plot of conversion *vs* time for benzyl alcohol **(a)** using **Cu A (b)** using **Cu B**

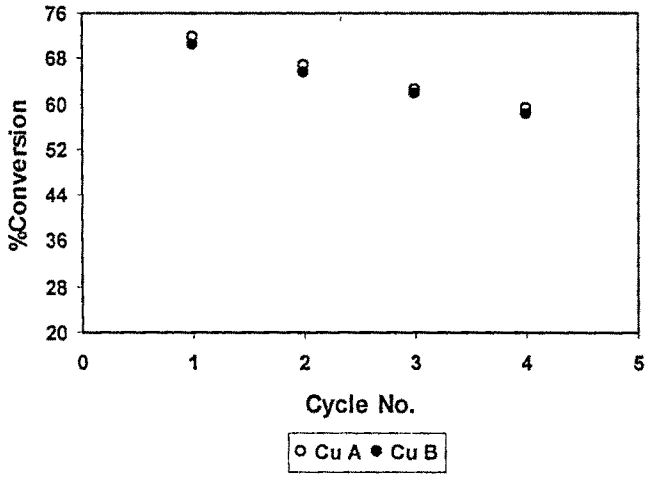

Fig. 3.3.8 Profile of catalyst recycle.

3.4. Mechanism of oxidation/epoxidation

It has now been well recognized that the metal catalyzed oxidation/epoxidation of alkanes/alkenes in presence of alkyl hydroperoxides can proceed *via* two distinctly different mechanisms; one involving a high valent metal oxo/peroxo species and the other involving free radical intermediates [39]. The two pathways are shown in **Scheme 3.4.1.** In order to gain some insight into the nature of the reaction catalyzed by these supported metal complexes a series of experiments were carried out using a free radical trap, 2,6-di-*tert* butyl-4-methyl phenol (BHT) and CCl_4 in the epoxidation of styrene and norbornylene by **Mn A** & **Ru A**, oxidation of cyclohexane by **Ru A** , benzyl alcohol & cyclohexane using **Cu A** & **Cu B**. It is known that BHT scavenges peroxy free radicals suppressing the yield of epoxide by radical autoxidation process (reaction proceed *via* free radical pathway) [40]. These results are summarized in **Table 3.4.1.** BHT (25 and 50 equivalents) was added to the reaction mixture *prior* to addition of TBHP.

Polymer supported Mn catalysts

There is a substantial lowering of the yields of oxidation products in case of **Mn A**. In further test for free radical intermediates, experiments were conducted in presence of excess CCl_4. Analysis showed a *lowering* in yields for styrene (from 20.4% to 18.0 %) and norbornylene (from 11.1% to 2.5%) with 25 equivalent of BHT as well as with 50 equivalent of BHT (from 20.4% to 2.2% for styrene , from 11.1% to 0 for norbornene). The observed product pattern in all these cases allow us to rationalize the results by assuming a mechanism involving predominantly *free radicals* in oxidation reaction catalyzed by **Mn A** [41,42].

Polymer supported Ru catalysts

In the oxidation reaction catalyzed by **Ru A** overall yield was only marginally reduced from 20.2% to 18.9% with 25 equivalent of BHT with styrene but a significant reduction by 42% (*i.e.* 30.7% to 17.7%) was observed for norbornylene. At higher concentrations of BHT (50 equiv.) yields were lowered by 32% for styrene but complete inhibition of products was found in case of the bicyclic olefins. As mentioned earlier in section 3.1., no oxidation was observed in presence of pure O_2 gas, indicating its non-involvement in the reaction. In subsequent tests for free radicals, experiments were conducted with CCl_4. Analysis showed partial reduction in yields for styrene as well as norbornylene but no other free radical induced side products *viz.* cyclohexyl chloride or bicyclohexyl were detected [42]. Results obtained in the oxidation reaction of cyclohexane again indicated marginal reduction in yields by 8.8% with 25 equivalent of BHT in the reaction with cyclohexane and at higher concentrations of BHT (50 equiv.) yields were reduced by 23.1%.

Based on these mechanistic probes it is possible to predict that the *major* route for the formation of different products is *via* a heterolytic cleavage of peroxide bond. Nevertheless, the partial suppression of reaction by radical traps even under high concentration points to the existence of free radicals. Such dual mechanistic pathways *i.e.* one proceeding in a heterolytic manner (*via* Ru(VI) or Ru(IV) oxo species) and the other by radical auto oxidation process essentially leading to the same products has also been suggested by earlier workers [42-46].

Polymer supported Cu catalysts

From the results compiled in **Table 3.4.1.** it is evident that there is no substantial drop in the yields of oxidation products in the reaction catalyzed by **Cu A & Cu B** in presence of BHT (50 equivalent) and CCl_4. These results allow us to envisage that the major route for the formation of different products is *via* a heterolytic cleavage of peroxide bond. Nevertheless, further study is essential to unambiguously prove the involvement of metal in higher oxidation state in these systems.

Table 3.4.1. Effect of free radical trap on oxidation[a]

Catalyst	Substrate	Additive	Additive : Catalyst (mole ratio)	Yield (%)	Yield (%) *without additive*
Mn A	Styrene	BHT	25	18.0	20.4
Mn A	Styrene	BHT	50	2.2	20.4
Mn A	Styrene	CCl_4	Excess	19.0	20.4
Mn A	Norbornylene	BHT	25	Trace	11.1
Mn A	Norbornylene	BHT	50	nil	11.1
Mn A	Norbornylene	CCl_4	Excess	5.7	11.1
Ru A	Styrene	BHT	25	37.8	40.4
Ru A	Styrene	BHT	50	27.4	40.4
Ru A	Styrene	CCl_4	Excess	28.4	40.4
Ru A	Norbornylene	BHT	25	17.7	30.7
Ru A	Norbornylene	BHT	50	nil	30.7
Ru A	Norbornylene	CCl_4	Excess	9.0	30.7
Ru A	Cyclohexane	BHT	25	16.6	18.2
Ru A	Cyclohexane	BHT	50	14.3	18.2
Ru A	Cyclohexane	CCl_4	Excess	14.0	18.2
Cu A	Benzyl alcohol	BHT	50	26.4	30.8
Cu B	Benzyl alcohol	BHT	50	26.4	30.0
Cu A	Cyclohexanol	BHT	50	12.8	12.8
Cu B	Cyclohexanol	BHT	50	10.8	11.2

a = temp. 28 °C; solvent = CH_3CN (20 ml); oxidant = TBHP; time = 24 h;

(a) **Homolytic cleavage :**

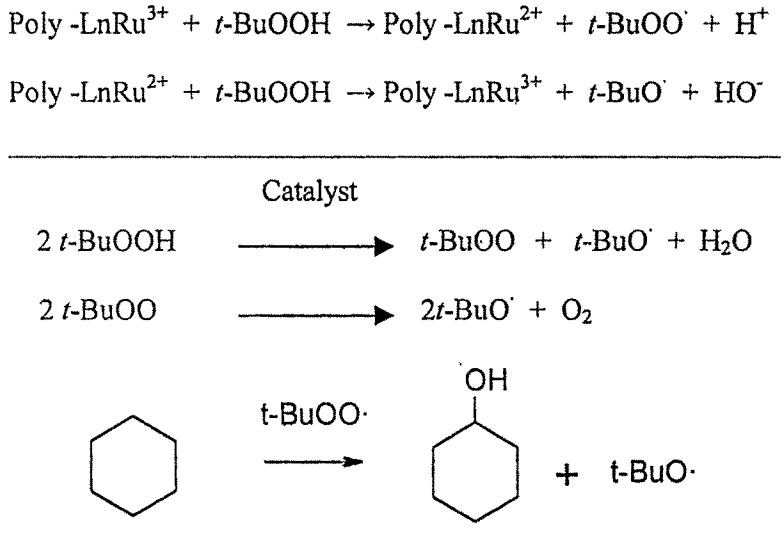

(b) **Heterolytic cleavage :**

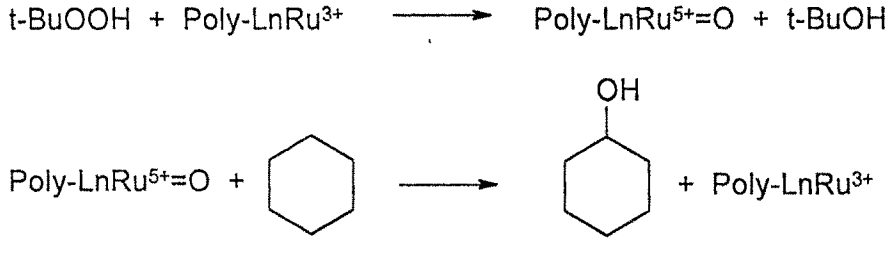

Scheme 3.4.1. Proposed mechanism of oxidation.

3.5. Asymmetric epoxidation of unfuctionalized aliphatic olefins by polymer supported amino acid metal complexes

Supported Mn(II) & Ru(III) catalysts:

1-octene (1-C_8) was initially subjected to asymmetric epoxidation with all the catalysts (**Mn A-Mn C**; **Ru A-Ru C**) in presence of *m*-chloro perbenzoic acid (*m*-CPBA) (**Table 3.5.1.**). Generally, high conversions (92-98%) were obtained in the temperature range 6°C – 40°C. Selective epoxide formation was observed irrespective of the nature of the metal complex. Expectedly , in the absence of the catalyst *m*-CPBA reacts with the substrate in a *non*-catalytic way under similar conditions giving only the *racemic* product. This means that the observed enantio-selectivity is due to the involvement of supported metal complex in the catalytic runs. The results obtained indicate that Mn(II)-amino acid complexes **Mn A-Mn C** exhibit higher enantiomeric induction (% ee : 20-38, entry 1-9) compared to Ru(III)-amino acid complexes **Ru A-Ru C** (% ee : 8-17, entry 10-18). To our surprise lower temperature lead to lower % ee for all catalysts.

To determine the *steric* effects on selectivity as well as %ee a series of aliphatic olefins such as 1-hexene (1-C_6), 2-methyl-1-pentene (2MP1), 4-methyl-1-pentene (4MP1) were examined using **Mn C** and **Ru C** catalysts at room temperature. Though excellent conversions were observed for all substrates (**Table 3.5.2.**, entry 1-8) with **Mn C** & **Ru C** lower %ee and selectivity to the epoxide were observed with **Ru C**. The reactivity pattern with either catalyst followed the order 4MP1<2MP1≈1-C_6<1-C_8. Optimum %ee were obtained at room temperature and remained unaffected up to about 40°C (entry 2,3,5,6; **Table 3.5.1.**).

In order to understand the efficacy of the present polymer supported **Mn C** catalyst vis-à-vis its *homogeneous* counterpart namely Mn(L-phenyl alanine)$_2$ an attempt was made to generate *in situ* (without isolation) a simple L-phenyl alanine complex of Mn(II) by mixing the ligand and the metal acetate in 1:2 molar ratio in an aqueous solution at a pH of ~4.1. After a reaction period of 24 h an aliquot of the solution corresponding to a Mn concentration equal to that employed in the supported catalyst was taken up for subsequent asymmetric epoxidation reaction with 1-octene in presence of *m*-CPBA under identical conditions. The % ee was nearly comparable (36% at 25°C) with that for the supported catalyst (38%).

Recycling experiments were conducted using 1-octene as a model substrate with **Mn C** and **Ru C**. Even after four catalytic cycles high conversions (93-97%, **Table 3.5.6.**) were obtained, though the enantioselectivity was slightly lowered under these conditions.

Mechanistic aspects

By far the most important advances in the asymmetric epoxidation of olefins have focused on metalloporphyrin catalysts (N_4 ligand) [47,48] and subsequently metallo-salen catalysts (N_2O_2 ligand) [49-51]. Yet another type of chiral epoxidation catalyst having N_2O_2 core structure is the β-ketoiminato complexes reported by Mukaiyama [52]. In our complexes the α -amino acid behave as an ' N_2O_2' donor ligand by forming a chelate with Mn(II) or Ru(III) ions though the ring size will essentially be smaller than in Schiff base or β-ketoiminato complexes. While the metallo-salens are known to induce very high enantioselectivity in asymmetric epoxidation of unfuctionalized olefins such as

styrene and its derivatives they have so far not been effective for simple olefins like 1-octene. The reason for poor activity of Schiff base metal complexes towards terminal olefins is not clearly understood. Amino acid complexes employed in the present work adopt a more or less planar stereochemistry around the central metal as in case of Schiff bases but may have an advantage over the latter complexes in incorporating stereogenic centers much closer to the metal (**Fig. 3.5.1**). This feature may facilitate the mode of oxygen transfer from the catalytically active oxo-metal species to terminal olefins such as 1-octene or 1-hexene. The stereo selective formation of products can be explained using simplified Groves – Jacobsen type of mechanism [53] involving concerted as well as a stepwise (*via* carbocation/radical) pathway (**Scheme 3.5.1**). The initially formed oxo-complex (*A*) reacts with 1-octene to form reactive intermediates (*B*) or (*C*) which rearranges to a C-O bond forming transition state (*D*). Finally through a concerted step the desired epoxide is obtained. If the intermediate (*D*) were to produce the epoxide directly and the starting catalyst back, one would expect 100% enantio induction. However, this is not the case as found by our experiments. These results indicate that a concurrent pathway exists in which interaction between the catalyst and olefin in presence of *m*-CPBA leads to a *racemic* product probably by auto oxidation or through the well known homolytic cleavage by peroxy radicals [54].

Branched olefins such as 2MP1 and 4MP1 epoxidize with considerably reduced %ee (**Table 3.5.2.**, entry 3,4,7,8) compared to straight chain olefins 1-octene and 1-hexene (entry 1,2,5,6). It is by now accepted that in the case of metal-salen complexes electron donating substituents on the ligand led to higher level of asymmetric induction [55] for terminal olefins with aryl groups at low temperature using *m*-CPBA and a donor.

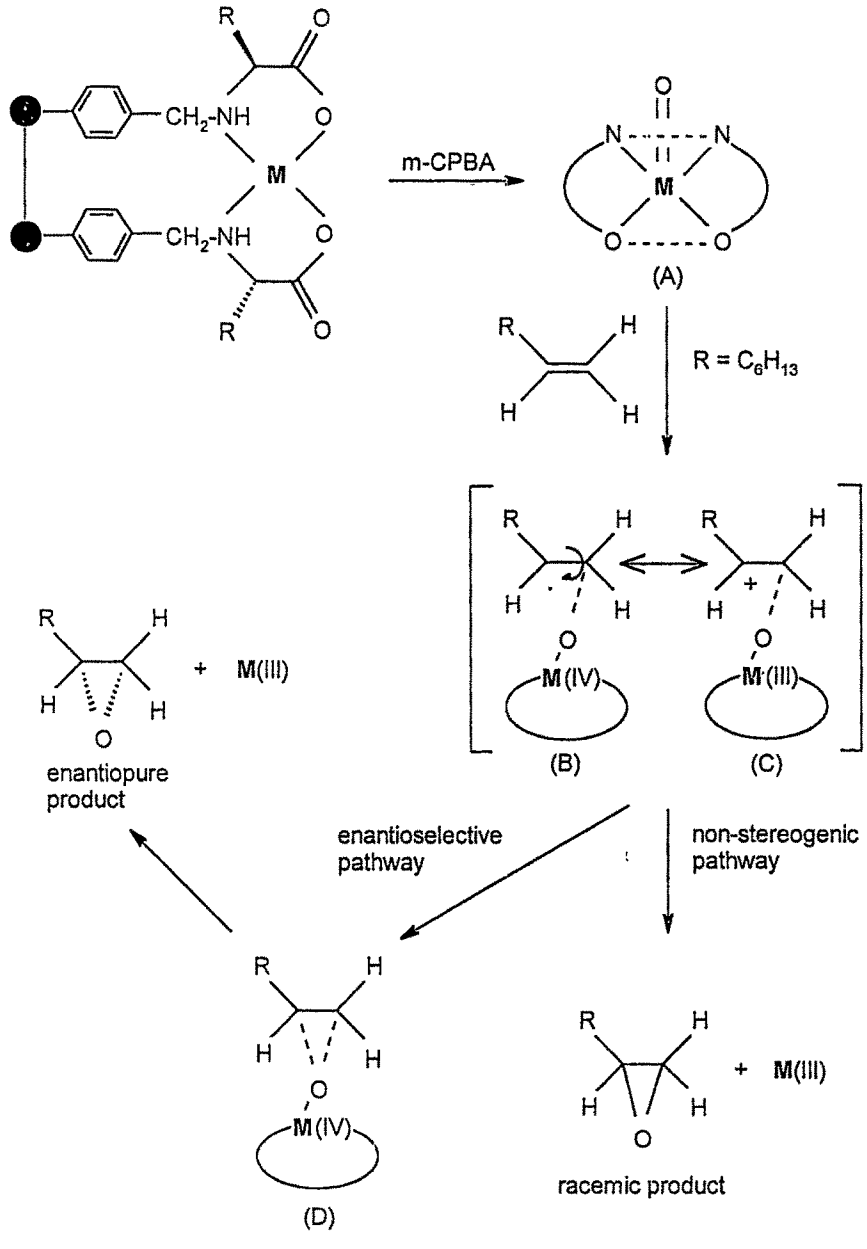

Scheme 3.5.1 Mechanism for asymmetric epoxidation.

In the present polymer supported amino acid complexes at lower temperatures diffusion limitation of substrate appear to contribute to the lowering of %ee. Nevertheless at 25°C, the observed enantioselectivity with **Mn C** is by far the *highest* achieved so far with non-Schiff base polymer anchored catalysts [56,57]. Interestingly both L-valine and L-phenyl alanine supported complexes show similar reactivity pattern. The activity is however, much pronounced for Mn(II) than for Ru(III). We perceive that though salen and amino acid complexes may have certain structural similarities as far as coordination geometry is concerned, there is a marked difference in the reactivity of the two types of ligands and their oxidation behaviour.

Apart from the catalyst structure and the nature of active species another critical factor which determines enantioseletivity is the structure of substrate olefin and its trajectory of approach towards the catalyst. As already discussed earlier with regard to the catalyst structure the amino acid complexes can be assumed to be similar to the planar Schiff-base Mn complex core (**Fig. 3.5.1**).

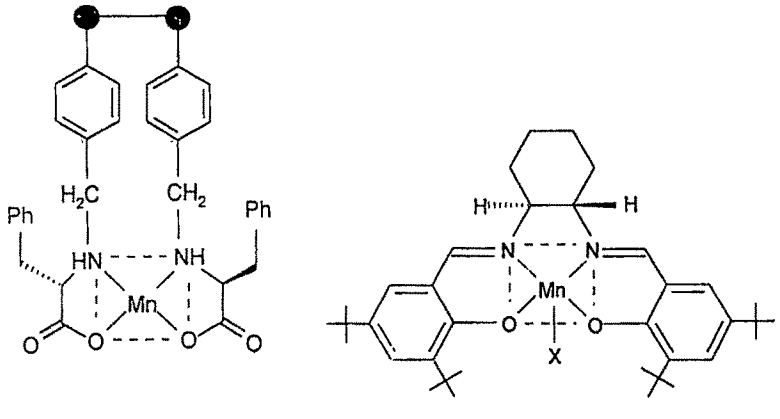

Fig. 3.5.1 Structure of **Mn C** and chiral Mn-Schiff base.

Following interaction with *m*-CPBA, two electron oxidation leads to high valent oxo-species (**Scheme 3.5.1**). The incoming olefin can attack the metal-oxo bond in one of three possible directions, *viz.* side-on, inclined (along the Mn-N bond axis) or in a perpendicular (to Mn-N_2O_2 plane) trajectory (**Scheme 3.5.2**).

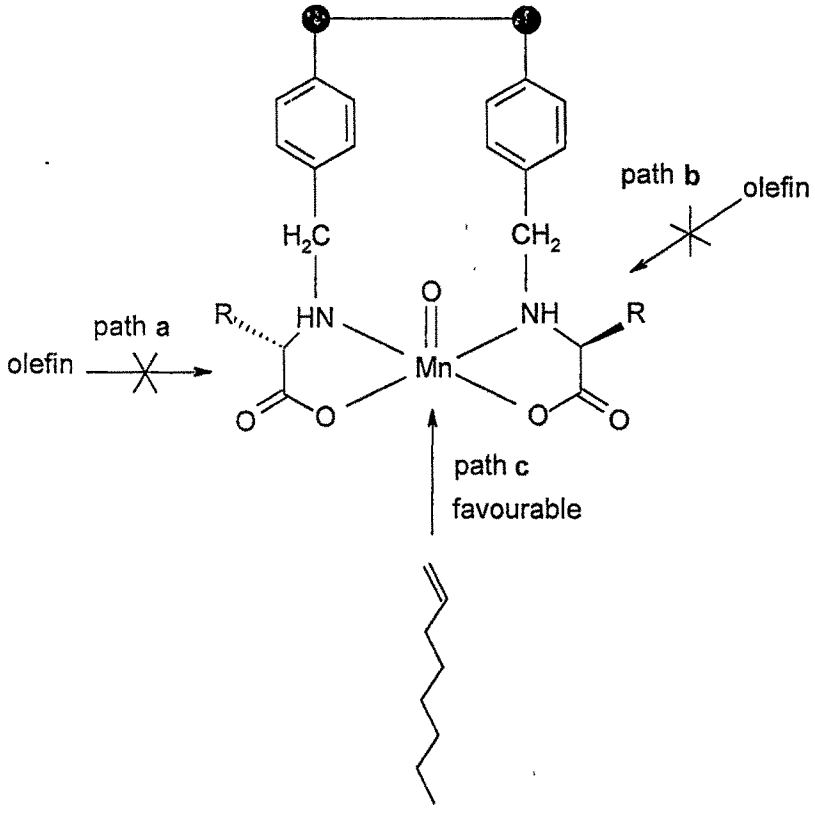

Scheme 3.5.2 Possible olefin trajectory to the Mn-oxo bond.

Orientation of the olefin along pathway **a** and **b** is expected to result in greater steric repulsion due to smaller size of the amino acid chelate as compared to the Schiff-base complexes[58,59]. Though there is not enough available information on steric effects imposed by the substrate on coordination geometry of Schiff base complexes, our results can best be rationalized using pathway **c** which is in tune with the model

suggested by Houk and co-workers [60] wherein the enantioselection was viewed as being provided by the chiral environment set up by transmission through the salen ligand of the effect of stereogenic carbons. Thus the observed %ee for 1-alkenes in our case though moderate, would be difficult to explain by pathway **a** or **b**. Indirect evidence in support of pathway **c** of olefin approach was obtained in the asymmetric epoxidation of styrene with **Mn C**. To our surprise only about 6% ee was observed under identical conditions. The bulky aryl substituent may pose steric constraints compared to the straight chain 1-alkenes leading to the observed differences in enantioselectivity. This also holds true for substituted 1-alkenes like 2-methyl-1-pentene and 4-methyl-1-pentene. Likewise structural differences between **Mn C** (four coordinate) and **Ru C** (hexa coordinate) can possibly account for the lowering in %ee during epoxidation with the latter catalyst. Further work is necessary to gain better insight into the mechanism of this reaction.

Table 3.5.1. Enantioselective epoxidation of 1-octene catalyzed by polymer supported Mn & Ru complexes

Entry	Catalyst	Temp. (°C)	Convn.(%)	Epoxide selectivity (%)	e.e.(%)[a]
1	**Mn A**	6	97	93	21
2		25	97	91	38
3		40	98	91	36
4	**Mn B**	6	97	93	22
5		25	98	92	37
6		40	98	91	36
7	**Mn C**	6	96	92	21
8		25	97	92	37
9		40	97	91	35
10	**Ru A**	6	92	82	10
11		25	93	79	18
12		40	92	80	17
13	**Ru B**	6	93	82	8
14		25	92	80	16
15		40	92	79	16
16	**Ru C**	6	93	81	8
17		25	94	78	17
18		40	93	78	16

[a] Determined by GC using Chiraldex ATA capillary column.

Table 3.5.2. Asymmetric epoxidation of terminal olefins at 25°C

Entry	Catalyst	Substrate	Convn. (%)	Epoxide selectivity (%)	e.e.(%)[a]
1	**Mn C**	1-octene	97	91	38
2		1-hexene	98	94	26
3		2-methyl-1-pentene	98	94	24
4		4-methyl-1-pentene	97	91	20
5	**Ru C**	1-octene	93	79	16
6		1-hexene	96	83	18
7		2-methyl-1-pentene	96	80	17
8		4-methyl-1-pentene	94	76	12

Table 3.5.3. Recycling studies on Mn C & Ru C in asymmetric epoxidation of 1-octene

Catalyst	Cycle no.	Convn.(%)	Epoxide selectivity (%)	e.e.(%)
Mn C	1	97	91	38
	2	96	92	37
	3	97	91	32
	4	96	90	27
Ru C	1	94	79	17
	2	94	81	16
	3	92	80	14
	4	93	78	11

Supported Cu(II) catalysts:

Catalysts **Cu A - Cu C** were initially screened for asymmetric epoxidation of 1-octene in presence of *m*-CPBA at various temperatures in methylene dichloride as solvent (**Table 3.5.4.**). In our experiments irrespective of the type of optically active amino acid, very high conversions (94-98%) and epoxide selectivity (90-94%) were obtained with all the Cu-catalysts within the temperature range of 6°C-40°C (entry 1-8, **Table 3.5.4.**). As in the case of Mn & Ru catalysts the enantioselectivity was considerably reduced at lower temperature (entry 1,4,7). Aliphatic olefins such as 1-hexene (1-C_6), 2-methyl-1-pentene (2MP1) and 4-methyl-1-pentene (4MP1) were epoxidized at room temperature using **Cu C**. Results in **Table 3.5.5.** again indicated excellent conversions and selectivity. The reactivity pattern with this catalyst also followed the order 4MP1<2MP1≈1-C_6<1-C_8. Neither the cross-link density of the polymer back bone (6% & 8%) nor the nature of amino acid (L-valine or L-phenyl alanine) had any major influence on the enantioselectivity.

Recycling experiments with **Cu A** (Table 3.5.5.) indicated no change in conversion (96-98%) after 3 cycles while enantioselectivity decreased with successive recycling step.

Table 3.5.4. Enantioselective epoxidation of 1-octene catalyzed by polymer supported Cu complexes

Entry	Catalyst	Temp. (°C)	Convn.(%)	Epoxide selectivity (%)	e.e.(%)[a]
1	**Cu A**	6	96	94	17
2		25	98	94	32
3		40	98	92	30
4	**Cu B**	6	96	93	18
5		25	98	92	30
6		40	98	92	29
7	**Cu C**	6	94	94	16
8		25	97	92	32
9		40	98	92	29

[a] Determined by GC using Chiraldex ATA capillary column.

Table 3.5.5. Asymmetric epoxidation of terminal olefins with Cu C at 25°C

Entry	Substrate	Convn. (%)	Epoxide selectivity (%)	e.e.(%)[a]
1	1-octene	98	94	32
2	1-hexene	97	93	26
3	2-methyl-1-pentene	98	94	22
4	4-methyl-1-pentene	96	90	18

Table 3.5.6. Recycling of Cu C in asymmetric epoxidation of 1-octene at 25°C

Cycle no.	Convn.(%)	Epoxide selectivity (%)	e.e.(%)
1	98	94	32
2	98	92	30
3	96	91	27
4	97	90	22

3.6. References

[1] R.F. Hirsch, E. Gancher, F.R. Russo, Talanta, 17, **1970**, 483.

[2] V.S. Rogozhin, V.A. Davankov, I.A. Yamskov, V.P. Kabanov, Vysokomol Soedin B, 14, **1972**, 472.

[3] M.A. Petit, J. Jozefonvicz, J. Appl. Poly. Sci., 21, **1977**, 2589.

[4] R.V. Snyder, R.J. Angelici, R.B. Meck, J. Am. Chem. Soc., 94, **1972**, 2660.

[5] D.W.L. Sung, P. Hodge, P.W. Stratford, JCS, Perkin I, 1463, **1999**.

[6] S. Tangestaninejad, M.H. Habib, V. Mirkhani and M. Moghadam, J. Chem. Research (s), **2001**, 444.

[7] T. Mathew, M. Padmanabhan, S. Kuriakose, J. Apply. Poly. Sci., 59, **1996**, 23.

[8] T.W. Greene, editor. *Protective groups in organic synthesis.* New York: John Wiley & Sons., **1981**, 273.

[9] R. Quitt, J. Hellerbach, K. Vogler, Helv. Chim. Acta., 46, **1963**, 327.

[10] W.L. Scott, C. Zhon, Z. Fang, M.J. O'Donnell, Tetr. Lett., 38, **1997**, 3695.

[11] A. E. Martell, R. M. Smith, *Critical Stability Constants.* New York: Plenum, 5, **1982**.

[12] G. Wilkinson, R. D. Gillard, J. A. McCleverty, editors. *Comprehensive coordination chemistry.* Oxford: Pergamon., 1, **1987**.

[13]. R. D. Gillard, R. J. Lancashire, P. O'Brien, Trans. Met. Chem., 5, **1980**, 340.

[14] (a) K. Nakamoto, *Infrared and Raman spectra of inorganic and coordination compounds.* New York: Wiley, **1997**; (b) A.W. Herlinger, S.N. Wenhold, T.V. Long II, J. Am. Chem. Soc., 92, **1970**, 6474; (c) A.W. Herlinger, T.V. Long II, J. Am. Chem. Soc., 92, **1970**, 6481.

[15] A. B. P. Lever, *Inorganic electronic spectroscopy.* New York: Elsevier, **1984**.

[16] N. A. Law, M. Tyler, V. L. Pecoraro, Adv. Inorg. Chem., 46, **1999**, 305.

[17] B. S. Goodman, J. B. Raynor, *Adv. Inorg. Chem. and radiochem.*, 13, 135,362, **1970**.

[18] A. Deroche, I. Morgenstern-Badaran, M. Cesario, J. Gwilhem, B. Keita, L. Nadio, C. Houic-Levius, J. Am. Chem. Soc., 118, **1996**, 4567.

[19] E. Tiezze, J. Chem. Soc. Perkin Trans II., 7, **1975**, 769.

[20] R.A. Sheldon, M. Wallau, Isabel W.C.E. Arends and Ulf Schuchardt, Acc. Chem. Res., 31,**1998**, 485.

[21] C. Che, W. Tang, W. Wong, T. Lai, J. Am. Chem. Soc., 111, **1989**, 9048.

[22] R. A. Sheldon, Topics. Curr. Chem., 23, **1993**, 164.

[23] P. Neubold, B.P.C. Della Vedova, K. Wieghardt, B. Nuber, J. Weris, Inorg. Chem. 29, **1990**, 3355, and references therein.

[24] J.A. Broomhead, L.A.P. Kane-Maguire, J. Chem. Soc. (A), **1967**, 546.

[25] G.M. Bryant, J.E.. Fergusson, H.K.J. Powell, Aust. J. Chem. 24, **1971**, 257;275.

[26] J.E. Fergusson, P.F. Heveldt, J. Inorg. Nucl. Chem. 39, **1977**, 825.

[27] Y. Kurimura, E. Tsuchida, M. Kaneko, J. Polym. Sci. 9, **1971**, 3511.

[28] B.P. Sullivan, D.J. Sullivan, T.J. Meyer, Inorg. Chem. 17, **1978**, 3334.

[29] C. Bunker, R.S. Drago, D.N. Hendrickson, R.M. Richmann, S.L. Kessell, J. Am. Chem. Soc. 100, **1978**, 3805.

[30] J.A. Stanko, H.J. Peresie, R.A. Bernheim, R. Wang, P.S. Wang, Inorg. Chem. 12, **1973**, 634.

[31] R. Schneider, T. Weyhermiller, K. Wieghardt, Inorg. Chem. 32, **1993**, 4925.

[32] S.Perrier, T.C.Lau, J.K.Kochi, Inorg. Chem., 29, **1990**, 4190.

[33] D.T. Gokak, B.V. Kamath, R.N. Ram, J. Appl. Poly. Sci., 35, **1985**, 1528.

[34] D.T. Gokak, R.N. Ram, J. Mol. Catal. A: Chemical, 49, **1989**, 285.

[35] G. Wilkinson, R.D. Gillard, J.A. Mecleverty, Editors, *Comprehensive coordination chemistry.* Oxford: Pergamon, 5, **1987**.

[36] B.M. Weckhuysen, A.A. Verberckmoes, L. Fu, R.A. Schoonheydt, J. Phys. Chem., 100, **1996**, 9456.

[37] R. Lontie, *Copper proteins and copper enzymes*, Boca Raton, CRC press Inc., Vols: 1-3, **1984**.

[38] (a) B.A. Goodman, D.B. McPhail, H.K.J. Powell, J. Chem. Soc. Dalton Trans., **1981**, 822. (b) W.S. Kittl, B.M. Rode, J. Chem. Soc. Dalton Trans., **1983**, 409. (c) M.J.A. Rainer, B.M. Rode, Inorg. Chim Acta, 107, **1985**, 127.

[39] R.A. Sheldon, J.K. Kochi, *Metal catalyzed oxidations of organic compounds*, New York, Academic **1981**.

[40] J.D. Koola, J.K. Kochi, J. Org. Chem. 52, **1987**, 4545.

[41] J.E. Sarneski, D. Michos, H.H. Thorp, M. Didiuk, T. Poon, J. Blewitt, G.W. Brudvig, R.H. Crabtree, Tetr. Lett., 32, **1991**, 1153.

[42] K. Srinivasan, S. Perrier, J.K. Kochi, J. Mol. Catal. 36, **1986**, 297.

[43] R.A. Leising, Y. Zang, L.Que Jr., J. Am. Chem. Soc. 113, **1991** 8555.

[44] S. Menage, J.M. Vericent, C. Lambeaux, G. Chottard, A. Grand, M. Fontecave, Inorg. Chem. 32, **1993**, 4766.

[45] R.H. Fish, M.S. Konings, K.J. Oberhausen, R.H. Fong, W.M. Yu, G. Christou, J.B. Vincent, D.K. Coggin, R.M. Buchanan, Inorg. Chem. 30, **1991**, 3002.

[46] R.A. Sheldon, Topics in Curr. Chem. 23, **1993**, 164.

[47] (a) J.T. Groves, T.E. Nemo, R.S. Myers, J. Am. Chem. Soc. 101, **1979**, 1032. (b) J.T. Groves, W.J. Kruper, J. Am.Chem. Soc. 101, **1979**, 7613. (c) J.T. Groves, T.E. Nemo, J. Am. Chem. Soc. 105, **1983**, 5786-5791.

[48] B. Meunier, E. Guilmet, M.E. De Carvalho, R. Poilblanc, J. Am. Chem. Soc. 106, **1984**, 6668.

[49] K. Srinivasan, P. Michaud, J.K. Kochi, J. Am. Chem. Soc. 108, **1986**, 2309.

[50] R. Irie, K. Noda, Y. Ito, N. Matsumoto, T. Katsuki, Tetrahedron Lett. 31, **1990**, 7345.

[51] W. Zhang,; E.N. Jacobsen, J. Org. Chem. 56, **1991**, 2296.

[52] (a) T. Mukaiyama, T. Yamada, T. Nagata, K. Imagawa, Chem. Lett. **1993**, 327. (b) T. Nagata, K. Imagawa, T. Yamada, T. Mukaiyama, Chem. Lett. **1994**, 1259.

[53] (a) J.T. Groves and M.K. Stern, J. Am. Chem. Soc., 110, **1988**, 8628. (b) W. Zhang, N.H. Lee, E.N. Jacobsen, J. Am. Chem. Soc., 116, **1994**, 425.

[54] P.A. MacFaul, I.W.C.E. Arends, K.U. Ingold, D.D.M. Wayner, J. Chem. Soc., Perkin Trans. 2, **1997**, 135.

[55] (a) E.N. Jacobsen, W. Zhang, M.L. Güler, J. Am. Chem. Soc. 113, **1991**, 6703. (b) M. Palucki, P.J. Pospisil, W. Zhang, E.N. Jacobsen, J. Am. Chem. Soc. 116, **1994**, 9333.

[56] R. I. Kureshy, N. H. Khan, S. H. R. Abdi, S. T. Patel, P. Iyer, S. P. Dastidar, J. Mol. Catal. 160, **2000**, 217.

[57] R. I. Kureshy, N. H. Khan, S. H. R. Abdi, P. Iyer, S. T. Patel, Polyhedron 18, **1999**, 1773.

[58] E.N. Jacobsen, W. Zhang, A.R. Muci, J.R. Ecker, L. Deng, J. Am. Chem. Soc. 113, **1991**, 7063.

[59] (a) N. Hosoya, A. Hafakeyama, K. Yanai, H. Fuji, R. Irie, T. Katsuki, Synlett **1993**, 641. (b) T. Hamada, R. Irie, T. Katsuki, Synlett, **1994**, 479.

[60] (a), K.N. Houk, N.C. DeMello, K. Condroski, J. Fennen, T. Kasuga, in *Electronic conference on heterocyclic chemistry* (ECHET 96), eds. Rzepa, H.S.; Snyder, J.P.; Leach, C. The Royal Society of Chemistry, London, **1996** CA 127: 205196f (1997). (b) C.T. Dalton, K.M. Ryan, V.M. Wall, C. Bousquet, D.G. Gilheany, Top. Catal. 5, **1998**, 75.